chemosensors

MDPI

Review

Recent Advances in Electrochemiluminescence Emitters for Biosensing and Imaging of Protein Biomarkers

Lei Yang [1] and Jinghong Li [1,2,3,4,*]

[1] Key Laboratory of Bioorganic Phosphorus Chemistry & Chemical Biology, Department of Chemistry, Center for Bioanalytical Chemistry, Tsinghua University, Beijing 100084, China; ly1994@mail.tsinghua.edu.cn
[2] New Cornerstone Science Laboratory, Shenzhen 518054, China
[3] Beijing Life Science Academy, Beijing 102206, China
[4] Center for BioAnalytical Chemistry, Hefei National Laboratory of Physical Science at Microscale, University of Science and Technology of China, Hefei 230026, China
* Correspondence: jhli@mail.tsinghua.edu.cn

Abstract: Electrochemiluminescence (ECL) is a light-emitting process triggered by the high energy redox between electrochemically oxidized and reduced luminophores or some coreactive intermediate radicals, representing a blooming hot topic over decades with a wide variety of bioanalytical applications. Due to the superb sensitivity, ultralow background noise, specificity, ease of integration, and real-time and in situ analysis, ECL has been developed as a convenient and versatile technique for immunodiagnostics, nucleic acid analysis, and bioimaging. Discovering highly-efficient ECL emitters has been a promising subject that will benefit the development of sensitive bioanalytical methods with prominent potential prospects. To date, the interdisciplinary integrations of electrochemistry, spectroscopy, and nanoscience have brought up the continuous emergences of novel nanomaterials which can be flexibly conjugated with specific bio-recognition elements as functional ECL emitters for bioassays. Therefore, a critical overview of recent advances in developing highly-efficient ECL emitters for ultrasensitive detection of protein biomarkers is presented in this review, where six kinds of the most promising ECL nanomaterials for biosensing and imaging of various disease-related protein biomarkers are separately introduced with references to representative works. Finally, this review discusses the ongoing opportunities and challenges of ECL emitters in developing advanced bioassays for single-molecule analysis and spatiotemporally resolved imaging of protein biomarkers with future perspectives.

Keywords: electrochemiluminescence; emitter; biosensing; imaging; protein biomarkers

check for updates

Citation: Yang, L.; Li, J. Recent Advances in Electrochemiluminescence Emitters for Biosensing and Imaging of Protein Biomarkers. *Chemosensors* **2023**, *11*, 432. https://doi.org/10.3390/chemosensors11080432

Academic Editor: Ilaria Rea

Received: 29 June 2023
Revised: 29 July 2023
Accepted: 1 August 2023
Published: 4 August 2023

Copyright: © 2023 by the authors. Licensee MDPI, Basel, Switzerland. This article is an open access article distributed under the terms and conditions of the Creative Commons Attribution (CC BY) license (https://creativecommons.org/licenses/by/4.0/).

1. Introduction

Electrochemiluminescence (ECL) is an electrically stimulated chemiluminescencent event that involves the excitation of luminophores through efficient redox reactions along with light emissions [1–3]. Benefiting from the unification of the high sensitivity of chemiluminescence and spatiotemporal controllability of electrochemistry, ECL has been developed as a powerful technique that not only needs no external light excitation but also perfectly avoids high-power laser irradiation and auto-photoluminescence with a high signal-to-noise ratio and almost zero background signal [4,5]. The ECL principles have been explored for over half a century since the 1960s, which can be generally categorized into two types: annihilation and coreactant ECL mechanisms [6,7]. Both of these two mechanisms require the efficient conversion of electrical energy into radiative energy that can be further exported as readable signals by ECL analyzers [8]. Usually, coreactant ECL performs stronger ECL emission in narrower potential windows than the self-annihilation pathway, which has promoted the application scope of the ECL technique from fundamental research to

clinical diagnosis. Till now, coreactant ECL systems have stimulated the growing development of commercialized ECL instruments and facilities as powerful diagnostic tools in medical institutions.

As well known, ECL emitters with high luminous efficiencies play crucial roles in ECL analytical systems since their qualities directly dominated the signal transduction efficiencies of the developed biosensors [9]. With the developments of nanoscience and nanotechnology, more and more attractive nanomaterial-based ECL emitters have been developed for bioassays, which greatly enriched the existing pool of ECL luminophores where classic ECL reagents including highly ECL-active ruthenium complexes, luminol with its derivates and iridium complexes are the mainstream choices for commercialization and fundamental researches. Nanomaterials with merits of large specific surface areas, high conductivities, tunable optical properties, and excellent electrochemical activities have opened new possibilities for the explorations of newly patterned mechanism models, constructions of ultrasensitive biosensors, and novel single-cell bioimaging probes for ECL bioanalysis. Those nanomaterials with outstanding quantum efficiencies can be directly fabricated and employed as promising ECL emitters for signal transduction or image probing. For those nanomaterials with large specific surface areas or porous nanostructures, such as mesoporous silica nanospheres (MSNs) [10–13], multiwall carbon nanotubes [14–16], graphene oxide [17–20], Ti_3C_2 MXene [21–23], and Au nanoparticles (NPs) [24], they can be utilized as the carriers to stabilize luminophores and developed as ECL emitters for biosensors. Unlike self-annihilation ECL pathway, a proper coreactant reagent is essentially required for coreactant ECL since it can generate abundant electro-active intermediates to promote the production of excited states, thus achieving stronger ECL intensity [25–27]. Instead of being carriers, nanomaterials with excellent electrical conductivity, electrochemical and catalytic activities can be utilized as coreaction accelerators to facilitate electron-transfer during the oxidation/reduction of coreactants to produce more radical intermediates, thus obtaining better signal amplification and higher sensitivity [28–30].

By virtue of the unique combination of ECL emitters with biorecognition elements such as antibody, nanobody, DNA, and aptamer, various ECL transducers have been established for ECL immunoassay, nucleic acid analysis, and cell imaging [7,31–33]. Biomarkers, considered as quantifiable indicators for some certain biological states of human bodies, hold enormous potential in diagnosing various severe diseases to human health [34,35]. Protein-based biomarkers are recognized as golden indicators for diagnosing various cancers such as carcinoembryonic antigen (CEA) [36–38], prostate-specific antigen (PSA) [39–41], alpha fetoprotein (AFP) [42,43], mucin 1 (MUC1) [44–46], and cytokeratin 19 fragments (CYFRA 21-1) [47–49]. Benefiting from the remarkable intrinsic features of ECL technique, more and more novel ECL nanomaterials have been diversely prepared and biofunctionalized as novel ECL emitters for detecting protein biomarkers of different diseases [33,50].

This review aims to provide a fresh summarization of key advances in the delicate fabrication of different kinds of novel nanomaterial-based ECL emitters along with developed biosensing and imaging strategies for analyzing protein biomarkers from cancers and non-cancer diseases. First, the recently reported novel nanomaterial-based ECL emitters were classified into different categories including quantum dots (QDs), metallic nanocrystals (MeNCs), metal–organic frameworks (MOFs), covalent organic frameworks (COFs), hydrogen-bonded organic frameworks (HOFs), and polymer dots (Pdots). Then, the most advanced sensing methods including self-enhanced ECL, aggregation-induced ECL (AIECL), ratiometric assay, ECL-resonance energy transfer (ECL-RET), or quenching-typed ECL biosensors are summarized, followed by a brief but informative sketch of recent advancements in ECL microscopy (ECLM) techniques for membrane imaging of protein biomarkers. In the final section, the ongoing challenges and opportunities are carefully addressed with future perspectives for readers as well. Though this review was delicately organized as comprehensively as possible, the readers are still suggested to refer to other excellent reviews and those unintentionally uninvolved works out of this review to deepen the understanding of current advances and future trends in the ECL domain.

2. Nanomaterial-Based ECL Emitters

To date, the family of ECL emitters has been expanded from classical ECL reagents such as $Ru(bpy)_3^{2+}$ and luminol to advanced nanomaterial-based emitters such as QDs, MeNCs, MOFs, COFs/HOFs, and PdotsQDs, MeNCs, MOFs, COFs, HOFs, and Pdots. It is worth noticing that the above six kinds of nanomaterial-based ECL emitters can be recategorized into two major types: inorganic and organic ECL emitters. Obviously, QDs and MeNCs belong to the inorganic ECL emitters while the other four kinds including MOFs, COFs, HOFs, and Pdots belong to the organic ECL emitters. As for the latter type of organic ECL emitters, more specific types can be classified considering the complexities in their structural components during preparation. For instance, the ECL emission in MOFs can be further categorized into three main pathways, such as guest-encapsulation in MOFs induced by ECL, ligand-induced ECL in MOFs, and metal ion-induced ECL in MOFs [51–53]. In this section, efforts are made to cover every sub-type of each kind of nanomaterial as much as possible along with representative and elegant examples that have been recently published and mostly cited to date.

2.1. Quantum Dot-Based ECL Emitters

Quantum dots (QDs), as one type of zero-dimensional nanomaterials, have been variously developed as attractive participators for photocatalysis, cell imaging, light-emitting diodes, and biosensors by virtue of their structural, optical and electrical properties, high photoluminescence quantum yields (QY), excellent luminesce stability, ease of hybridizing with other components, and so on [54–57]. The first nonaqueous ECL study of silicon QDs was reported in 2002 [54]. After that, a wide variety of III-V and II-VI QDs including Cd-based QDs, Mo/W/Sn-based QDs, carbon QDs, and perovskite QDs gradually emerged as promising ECL luminophores. As previously reviewed by Zhou et al. [55], the ECL mechanism for QDs normally involves high-energy electron transfer along with the formation of radicals to generate pure ECL emission via the self-annihilation and coreactant pathways. Cd-based QDs include CdSe [56,57], CdS [58,59], CdTe [60–62], and core-shell CdTe@ZnS QDs [63]; CdSe@ZnS [64] have been exploited as ECL emitters in the last decade since this family usually owns narrow emission and size-dependent ECL with high stability in the aqueous phase and an ease of surface modification with other components. The hybridization of Cd-based pure QDs with other beneficial nanomaterials have been investigated for promoted ECL behaviors. For example, Liu et al. [65] recently prepared CdS QDs hybridized porphyrinic Zr-MOFs (PCN-224/CdS QDs) as cathodic ECL emitters for Sa-16S rDNA detection using $K_2S_2O_8$ as the coreactant. It was claimed that the electro-active PCN-224 with large specific surface area not only provided abundant sites to anchor CdS QDs stably but also functioned as a coreaction accelerator to facilitate the reduction of $S_2O_8^{2-}$ for ECL amplification, thus achieving a high detection sensitivity. However, Cd-based QDs showed limited applicability due to the environmental toxicity, complex preparation process, and poor biocompatibility [66]. To satisfy the demand of biological applications, outer-capping by a biocompatible shell on the external surface of Cd-based QDs has been developed as a doable solution to improve the biocompatibility. Pan et al. [67] prepared SiO_2-capped CdTe QDs hybrids (SiO_2@CdTe) as ECL emitters for biosensor construction. The SiO_2@CdTe showed a lowered cytotoxicity due to the encapsulation of the biocompatible SiO_2 shell, which endowed the biosensor a better performance for biological detection. Otherwise, some attractive QDs such as SnS_2 [68,69] MoS_2 [70], EuS [71], AgBr [72], SnO_2 [73], and black phosphorus (BP) [74,75] QDs containing no heavy-metal elements have also been developed as ideal alternatives for Cd-based QDs. As previously reported, Lei et al. [69] developed a green hydrothermal method to prepare heavy metal-free SnS_2 QDs which showed favorable cathodic ECL emission using $S_2O_8^{2-}$ as the coreactant. To achieve stronger ECL signals of SnS_2 QDs, Li et al. [76] used polyethyleneimine (PEI) functionalized titanium dioxide hollow spheres (THS) to stabilize large amounts of SnS_2 QDs, the formed hybrids exhibited stronger ECL emission for ultrasensitive detection of chloramphenicol. Hua et al. [71] first revealed the cathodic

ECL property of EuS QDs whose emission can be specifically quenched by Hg^{2+}, based on which, a facile and sensitive Hg^{2+} sensor was developed for seafood monitoring. Recently, Yu et al. [74] discovered a dual excited states-dominated ECL mechanism of the BPQDs prepared with an average size of 4 nm (Figure 1A). The surface oxidation defects of BPQDs were effectively passivated by externally modified arginine (Arg) moieties. It was highlighted that the electron transition channels of BPQDs can be modulated by those Arg moieties to generate significantly enhanced ECL emission using $K_2S_2O_8$ or $N_2H_4{\cdot}H_2O$ as the coreactant (Figure 1B). Moreover, Arg moieties endowed BPQDs with greatly improved biocompatibility, thus BPQDs were applied as ECL emitters for the sensitive analysis of integrin inhibitors on cell surfaces, resulting in a well-evaluated inhibiting efficiency. New synthetic strategies have been exploited to fabricate ECL-active multinary QDs such as AgGaInS QDs [77], $CuInS_2$/ZnS QDs [78], and ZnAgInS/ZnS [79] through efficient interfacial engineering on the interior inorganic structures and inorganic–organic interfaces, which also injected new insights for the developments and regulations of more highly-efficient QDs in ECL bioassays.

Benefiting from the low toxicity, good biocompatibility, sturdy chemical inertness, and easy of functionalization, carbon-based QDs including carbon QDs (CQDs), graphene QDs (GQDs), Ti_3C_2 MXene QDs, and graphitic carbon nitride QDs (g-CNQDs) have gained considerable attention as a class of promising ECL emitters for bioassays [66,80]. With the aim of improving the ECL efficiency of pure CQDs, nitrogen (N) doping was observed as an efficient strategy to lower the oxidation potential of CQDs with a significantly boosted anodic ECL emission. Chen et al. [81] prepared N-doped CQDs by a solvothermal method (Figure 1C). It was found that after lots of N atoms were doped into the graphitic cores of CQDs, which promoted positive shift of highest occupied molecular orbital (HOMO) to an upper energy level, thus achieving a 2.5-fold increased ECL efficiency at a rather low excitation potential of +0.11 V. Meanwhile, efforts such as the co-doping of multi-atoms have also been devoted to enhancing the ECL efficiency of pristine CQDs. Chen et al. [82] prepared biocompatible and water-dispersive nitrogen/sulfur (N/S) co-doped CQDs (NS-CQDs) by using cysteine and tryptophan as the precursors, which exhibited high photoluminescence QY of 73% for ECL application. In addition, Liu et al. [83] prepared highly electronegative fluorine/nitrogen (F/N) co-doped CQDs (FN-CQDs) via a one-step solvothermal method for HIV DNA fragment detection (Figure 1D). Since phosphorus (P) possesses a larger atom radius with a higher electron-donating ability than N, it can potentially be used as a dopant for CQDs to improve the ECL efficiency. Therefore, Yang et al. [84] developed the P/N co-doped CQDs (P/N CQDs) as efficient ECL emitters which showed eight-fold enhanced ECL intensity than N-doped CQDs for the sensitive detection of the mutant BRAF gene.

2.2. Metal Nanocluster-Based ECL Emitters

Metal nanoclusters (MeNCs), entailing a metal core consisting of a few atoms protected by a peripheral ligand shell, have become a scientific interest in the ECL domain over the last decade due to the merits of their molecule-like structure, intense quantum size effect, tunable luminescence, stable electronic and physicochemical properties, good electrocatalytic activity, and low biotoxicity [85–87]. Chemical reduction and electrochemical reduction have been the most used preparation methods for ECL-active MeNCs which usually involve the formation of a metallic core capped by a shell made of thiol ligands such as glutathione (GSH), 3-mercaptopropionic acid (MPA), and dithiothreitol (DTT) [87]. In 2009, the pioneering work on MeNCs was conducted by Díez et al. [88] who first revealed the tunable ECL emission of silver nanoclusters (Ag NCs). Since then, the fundamental knowledge of synthetic procedures and optimized ECL emission by ligand engineering on MeNCs has been gradually enriched. To date, monometallic, bimetallic. and MeNC-derived composites have become the three most investigated categories in the exploration of novel ECL-active MeNCs. Au NCs are the most well-known, popular, and representative monometallic MeNCs among such hot topics in the ECL realm. How to improve the

dispersion, stability, and quantum yield of Au NCs in the water phase is still a challenging issue. To embrace this challenge, Wang et al. [89] prepared self-enhanced Au NCs by the covalent conjugation of co-reactive *N*,*N*-diethylethylenediamine (DEDA) with Au NCs (Au-LA-DEDA). The well-matched redox activity between DEDA and Au NCs in one hybrid structure gave rise to significantly boosted ECL emission due to the shortened electron and mass transportations. Li et al. [90] and Fang et al. [91] successively investigated the cathodic and anodic ECL properties of BSA-stabilized Au NCs in aqueous media. Notably, the efficient external encapsulation of a layer of BSA shell endowed the pristine Au NCs with a well-improved water dispersity and stability for aqueous bioassay. In addition, Kim et al. [58] prepared glutathione-stabilized Au NCs which not only owned good dispersion and stability in water but also generated strong near-infrared ECL (NIR-ECL) emission for bioassays. Meanwhile, Peng et al. [59] prepared the methionine-capped Au NCs which performed strong anodic NIR-ECL emission with a dramatically increased ECL quantum yield of 66%. After that, the NIR-ECL Au NCs including Au_{18} [92], Au_{21} [93], and Au_{38} [94] NCs were comprehensively investigated by Ding's group. For example, Hesari et al. [93] prepared two $Au_{21}(SR)_{15}$ NCs of $Au_{21}^{hcp,0}$ and $Au_{21}^{fcc,0}$ whose electrochemistry behaviors and ECL mechanisms with tri-*n*-propylamine (TPrA) were studied in detail (Figure 2) which was quite informative for understanding the basic characteristics and ECL mechanisms of Au NCs with wide scopes of NIR-ECL applications.

The controllable formation of bimetallic NCs (BNCs) was reported as an effective strategy for ECL optimization of individual metallic counterparts due to the triggered synergetic effects [95]. To date, Pt [96], Pd [97], and Ag [98,99] have already been doped with Au NCs to form BNCs with boosted ECL emission and lower biological background interferences for biosensing than pristine Au NCs. Chen et al. [98] prepared rod-shape bimetallic $Au_{12}Ag_{13}$ NCs which exhibited 10-fold enhanced self-annihilation ECL efficiency and 400-fold enhanced coreactant ECL efficiency using $Ru(bpy)_3^{2+}$-TPrA as the reference. It was claimed that the ECL enhancements were attributed to the stabilization of charges on the LUMO orbital by the 13th Ag atom at the central position which made $Au_{12}Ag_{13}$ NCs more rigid in their core to reduce the nonradiative decays. Guo et al. [100] prepared well-confined ECL emitters of Au–Ag bimetallic NCs (Au–Ag NCs) capped by GSH stabilizers whose ECL emission was linearly and selectively enhanced by the exogenously added spermine, thus making Au–Ag NCs perfect ECL emitters for sensitive detection of spermine in practical applications.

Though ligand engineering or formation, bimetallic crystallization can effectively regulate the ECL efficiency of MeNCs; it is still challenging to endow them with a uniform distribution on substrates to decrease self-aggregation induced ECL quenching [101]. Therefore, conductive nanomaterials with large specific surface areas are employed as carriers to anchor MeNCs in a uniformly distributed manner; this has become a promising option to eliminate the ACQ effect. Previously reported works showed that Au NCs or Pt NCs can be anchored on the graphene oxides (GO) to act as luminous substrates for ECL detections [102,103]. Nie et al. [101] employed the GSH-protected Au NCs as building blocks that can assemble with Zn^{2+} to form the ECL-active Au NCs@ZIF-8 MOFs. It should be noted that the ordered distribution of Au NCs in MOF structure triggered a 10-fold stronger ECL emission than individual Au NCs in the water phase, thus a quenching-typed biosensor was constructed for the label-free detection of rutin with high sensitivity.

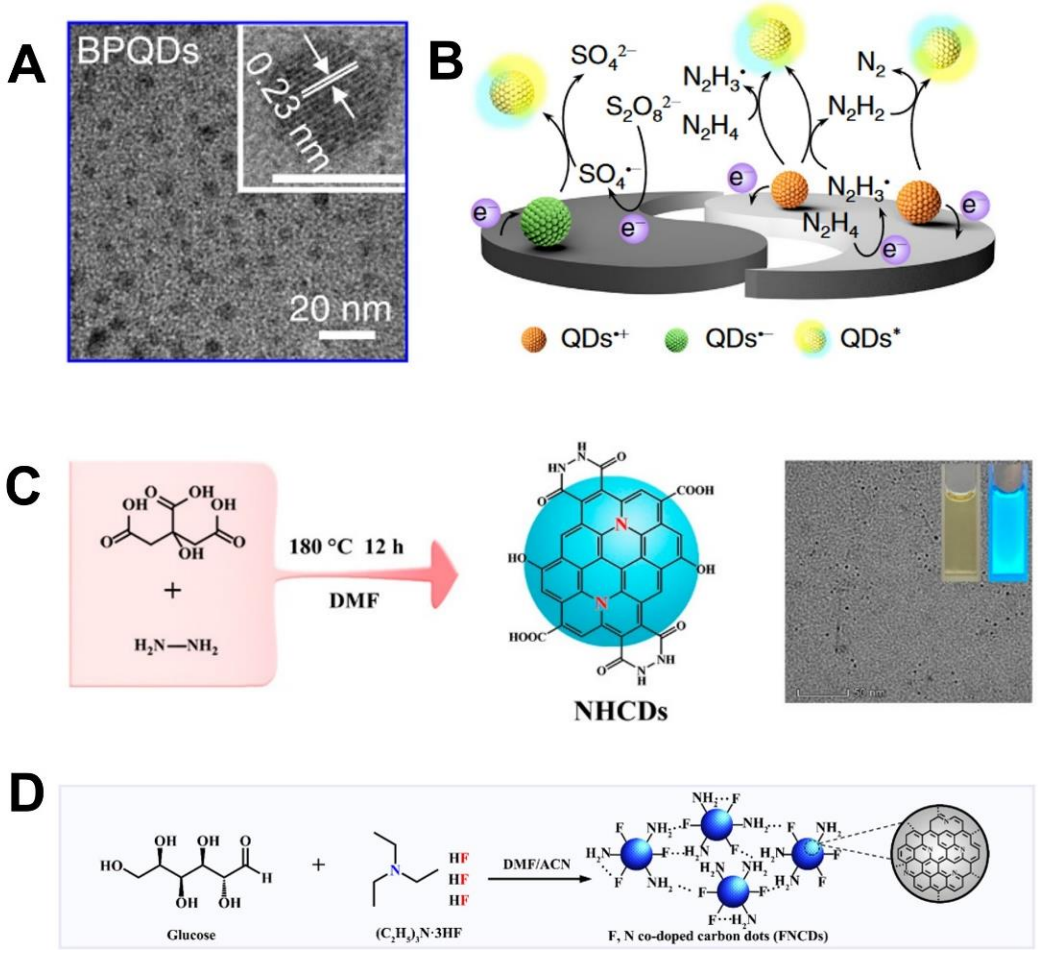


Figure 1. (**A**) Transmission electron microscopy image and high-resolution (inset) image (scale bar: 5 nm) of BPQDs; and the (**B**) cathodic and anodic ECL mechanisms for Arg-modified BPQDs/GCE using the $K_2S_2O_8$ and $N_2H_4{\cdot}H_2O$ as coreactants. Reprinted with permission from Ref. [74], Copyright 2022 Springer Nature. (**C**) Preparation of blue NHCDs. Reprinted with permission from Ref. [81], Copyright 2020 American Chemical Society. (**D**) Preparation of the FNCDs. Reprinted with permission from Ref. [83], Copyright 2023 Elsevier.

2.3. MOFs-Based ECL Emitters

Metal–organic frameworks (MOFs), as an emerging class of crystalline networks with high surface area and porosity, are formed by the ordered assembly of organic ligands with inorganic metal ions which have become promising candidates in chemical sensing, energy storage, adsorption and separation, catalysis, and luminescence [104,105]. Most of the members in the MOFs family can be further classified into three tailorable spatial dimensions (1D, 2D, and 3D) in terms of framework topologies and intricate skeletons [106]. To date, MOFs with different dimensions have been employed as carriers or scaffolds to stabilize ECL luminophores including $Ru(bpy)_3^{2+}$, luminol, and its derivatives as emitters for ECL biosensing applications [107]. To date, the feasibilities of UiO-66 [108], UiO-66-NH_2 [109], ZIF-8 [101], UiO-67 [110–112], MIL-101 [113], MOF-5 [114], PCN-222 [115], and PCN-777 [116] as carriers or scaffolds have been exploited; among these, Zr-based MOFs yield higher popularity due to their desirable physicochemical stabilities, porous features, and electrochemical activities [106]. Meanwhile, some Fe-/Co-based MOFs with enzyme-mimicing properties can catalyze the generation of ROSs for signal amplification of H_2O_2-based ECL systems [117–119]. In-depth studies were focused on how to conquer the unnecessary leakage of ECL luminophores from MOFs during real applications. One is to use those ECL luminophores as ligands to fabricate MOFs while the other one is to use

ECL-active metal ions to assemble with proper ligands. Until now, $Ru(bpy)_3^{2+}$ [110] and the derivatives of 9,10-di(pcarboxyphenyl)anthracene (DPA) [120], perylene [121], pyrene [122], porphyrins, and tetrakis (4-carboxyphenyl) porphyrin (TCPP) [123,124] have been served as ECL-active ligands to prepare MOFs. As a brave attempt, Zhu et al. [120] hired two different kinds of ligands to design a highly ECL emissive mixed-ligand MOF (m-MOF) in Figure 3A. These two ligands including DPA as a ECL luminophore and 1,4-diazabicyclo [2.2.2] octane (D-H_2) as the perfectly matched coreactant were well confined in the same reticular structure which was attributed to achieve a 26.5-fold ECL amplification via a newly demonstrated intra-reticular charge transition pathway (Figure 3B). Meanwhile, along with vigorous developments in aggregation science, aggregation induced emission (AIE) has injected new vitality into the preparation of highly-emissive ECL probes to avoid the unnecessary aggregation-caused quenching (ACQ) effect [125]. Reports also show that some planar AIEgens can serve as ligands whose intramolecular motions can be confined inside of rigid crystal MOF nanostructures to generate much stronger ECL emissions than their monomers, defined as aggregation induced ECL (AIECL) [126]. Notably, the AIE star molecule of tetraphenylethene (TPE) as well as its various derivatives of 1,1,2,2-tetra(4-carboxylbiphenyl)ethylene (H_4TCBPE) [45,125] and 1,1,2,2-tetrakis(4-(pyridin-4-yl)phenyl)-ethene (TPPE) [127] have all been explored as AIECL ligands to fabricate ECL-active MOFs for biosensing. As an attempt, Li et al. [125] prepared a green emissive Zr-MOF using the H_4TCBPE as AIECL organic ligands which was proved to perform an efficient coordination-triggered ECL (CT-ECL) emission that can be quenched by the AuPd@SiO_2 in a signal-off mode for sensitive immunoassays of neuron-specific enolase (NSE). A possible AIECL mechanism was mainly due to the restriction of intramolecular motions of H_4TCBPE in the rigid MOF matrix which efficiently reduced non-radiative decay for high ECL emission [126].

Recently, self-luminous lanthanide MOFs (Ln-MOFs) with unique antenna effects, a strong energy-transfer capability, and tunable luminescence properties are considered as promising ECL emitters for developing solid-state biosensors [107]. The pioneering studies on the luminescent Ln complexes were carried out by Bard et al. [128] in 1996. Ln^{3+} with a strong positive charge and large radius can collaborate with strongly absorbing organic ligands to display variable coordination configuration, thus increasing the structural tailor-ability and application scope of Ln-MOFs [129,130]. The so-called antenna effect in Ln-MOFs could be triggered when organic ligands absorb photons and act as an antenna to produce triplet states (T1) through intersystem crossing (ISC), sensitizing Ln^{3+} ions for ECL emission [48]. Different ECL-active lanthanide elements, including those already reported ones, namely Eu- [47,107,131–133], Ce- [45], Tb- [134–136], La- [137], and Yb- [138] based MOFs, have already been investigated for ECL applications. Until now, different Eu-based MOFs with excellent ECL properties were fabricated by sensitizing the Eu^{3+} with different ligands [47,107,131–133]. For example, Zhao et al. [47] prepared a mixed valence Eu-MOF by the coordination of $Sr(HCOO)_2$ ligands with Eu^{2+}/Eu^{3+} (Figure 3C). The antenna effect of the Eu-MOFs guaranteed the effective sensitization of $Sr(HCOO)_2$ toward Eu^{2+}/Eu^{3+}, thus generating high ECL efficiency by transferring the energy from the $4f^6 5d^1$ level of Eu^{2+} to the $^5D_0$ level of Eu^{3+} (Figure 3D). It is also quite innovative to design ECL-active Ln-MOFs with a self-triggered signal-amplification function by equipping some positive accelerators into the MOF structures. In addition, since the redox pair of Cu^{2+}/Cu^{+} can efficiently catalyze the reduction in coreactants of $S_2O_8^{2-}$ for ECL amplification, a hollow and porous Cu^{2+} doped Tb-MOF (Cu:Tb-MOF) was thus prepared by Wang et al. [136] as self-enhanced ECL emitters for sensitive immunoassays of pro-gastrin-releasing peptide (ProGRP) which indicated that introducing a redox-active pair such as Cu^{2+}/Cu^{+}, Ce^{3+}/Ce^{4+}, or Co^{3+}/Co^{4+} might be a potential and doable strategy to regulate and improve the ECL efficiency of Ln-MOFs for biosensing application.

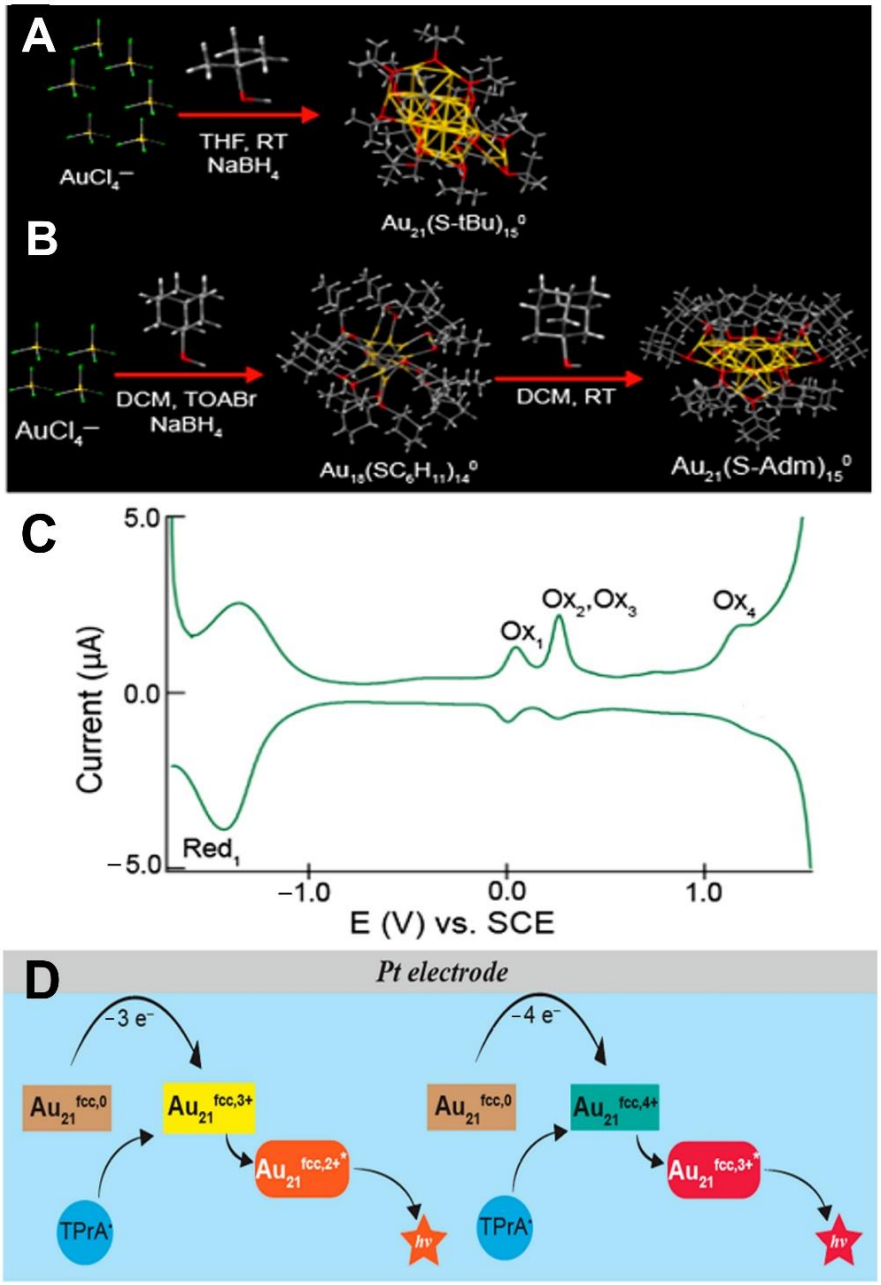


Figure 2. (**A**) One-step synthesis of $Au_{21}^{hcp,0}$. (**B**) Synthesis route of $Au_{21}^{fcc,0}$. (**C**) Differential pulse voltammograms (DPVs) of a 0.10 mM solution of $Au_{21}^{fcc,0}$ in dichloromethane containing 0.1 M $TBAPF_6$. (**D**) Anodic ECL mechanism of $Au_{21}^{fcc,0}$ on a Pt electrode. Reprinted with permission from Ref. [93], Copyright 2021 American Chemical Society.

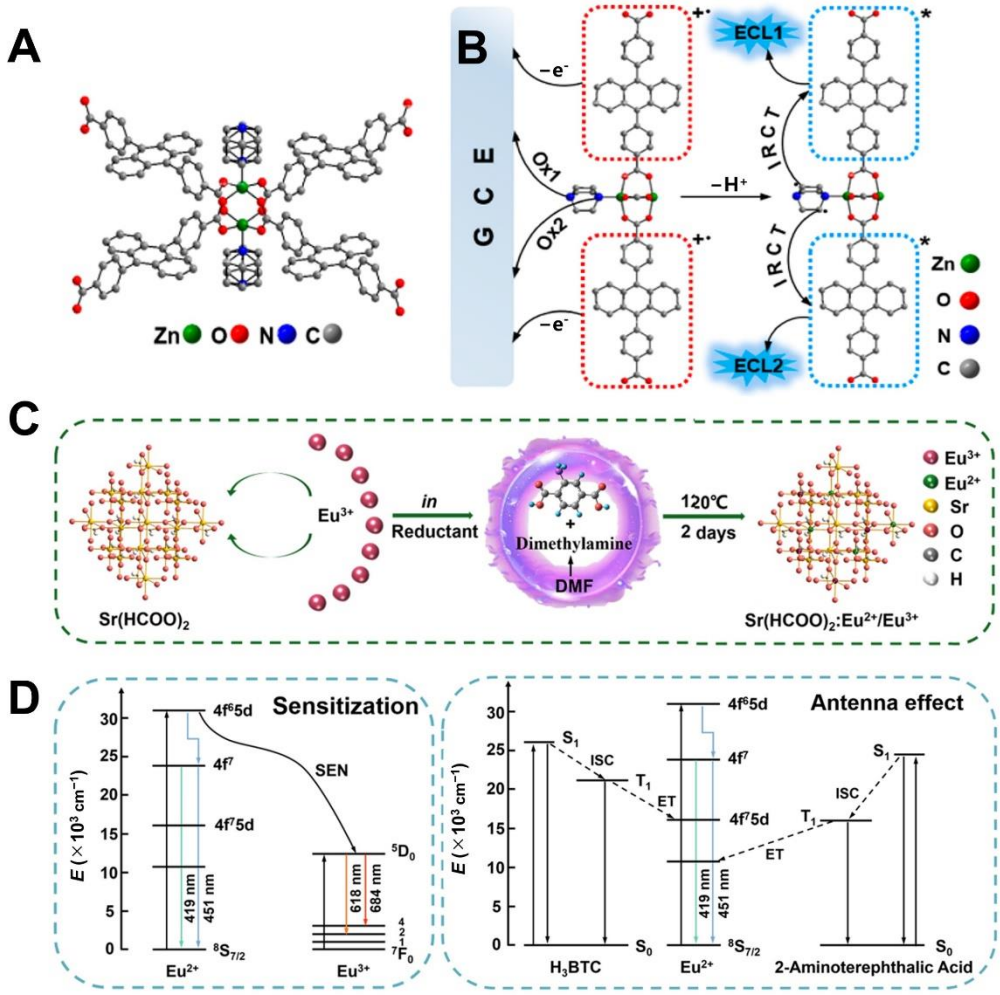


Figure 3. (**A**) Paddlewheel unit and (**B**) stepwise ECL mechanism of m-MOF via a dual intrareticular oxidation pathway. Reprinted with permission from Ref. [120], Copyright 2021 Springer. (**C**) The synthesis route of $Sr(HCOO)_2$:Eu^{2+}/$Eu^{3+}$and (**D**) simple models for the antenna effect of ligand to Eu^{2+} and the sensitization of Eu^{2+} to Eu^{3+}. Reprinted with permission from Ref. [47], Copyright 2023 Elsevier.

2.4. COFs/HOF-Based ECL Emitters

Though MOFs have gained considerable attention in the ECL domain, more and more concerns have been aroused from this hot topic, especially the underlying ECL quenching problem induced by the used metal ions or the ACQ effect of used planar ECL ligands [139,140]. By removing metal ions, covalent organic frameworks (COFs) have developed as a new class of fascinating metal-free crystalline porous ECL emitters which are attracting wide attention by virtue of their ultrahigh surface areas, favorable biocompatibility, adjustable porosity, and tunable physicochemical or luminescence activities that are on a par with MOFs [104,141]. Previous reports claimed that the ACQ effect of traditional planar luminophores in coordination polymers can be reduced or even eliminated by conjugation with AIEgens which will realize the ACQ-to-AIE transformation to obtain dramatically enhanced ECL emission [142]. Zhang et al. [143] reported a pyrene-based sp^2 carbon-conjugated covalent organic framework (COF) nanosheet (Py-sp^2c-CON) which was constructed by the C=C polycondensation of 2,2′-(1,4-phenylene)diacetonitrile (PDAN) and tetrakis(4-formylphenyl)pyrene (TFPPy). Topological attachment of TFPPy to PDAN in COFs can efficiently decrease the ACQ effect to fulfill an enhanced ECL efficiency. In addition, Luo et al. [144] designed the donor–acceptor (D–A) COFs with triphenylamine and triazine units which functioned by the tunable intrareticular charge transfer (IRCT)

in Figure 4A. The IRCT dominated dual oxidation was proved to be an efficient ECL mechanism which resulted in an approximate 123-fold ECL enhancement compared to the benzene-based COFs (Figure 4B). Meanwhile, Li et al. [145] developed a scalable method to design Olefin-linked donor- and acceptor-conjugated COFs where different donors and acceptors were restricted in different electron configurations, forming highly transferred intramolecular electronic networks for stronger ECL emission in the presence of no exogenous poisonous coreactants (Figure 4C). Cui et al. [146] assembled an electron-withdrawing monomer of 2,4,6-trimethylbenzene-1,3,5-tricarbonitrile (TBTN) into the COFs structures conjugated with electron-donating olefin molecules which endowed the non-ECL emissive TBTN monomer with a favorable ECL activity through efficient intramolecular electron-transfer mechanism. Similarly, Li et al. [147] used olefin-linked COFs to fabricate a highly aligned array substrate where donors and acceptors were co-crystallized and stacked into COFs structure. By using 2,4,6-trimethylbenzene-1,3,5-tricarbonitrile (TBTN) as the acceptor, tunable ECL emissions of different non-ECL donors were triggered in the formed electron freely-transported networks. For realizing better electrochemical behavior, the poor conductivity of COFs were carefully dealt with in the following studies. For instance, Zhang et al. [148] prepared a conductive COF by using two large π-conjugated planar ligands of 2,3,6,7,10,11-hexahydroxytriphenylene (HHTP) and 2,3,6,7,10,11-hexaaminotriphenylene (HATP) as dual ECL luminophores. The formed conductive porous framework of HHTP-HATP-COF performed significantly improved electronic conductivity and accelerated the mass–transport ratio, resulting in strong cathodic ECL emission along with outstanding aqueous stability.

In addition to MOFs or COFs, hydrogen-bonded organic frameworks (HOFs) are another vibrant class of crystalline porous ECL emitters based on the non-covalent hydrogen-bonding interaction. The building motifs of HOFs usually contain scaffolds covered with abundant hydrogen-bonding interacting sites and some linkers to form rigid HOF backbones [149–151]. Due to the high electrochemical activity and π–π interaction propensity in those HOFs networks, the IRCT efficiency for amplifying ECL emissions can be guaranteed by efficient electron coupling effect [151]. For example, Hou et al. [151] reported two HOFs (HOF-100 and HOF-101) which were separately prepared by using 1,3,6,8-tetracarboxy pyrene (TCPY) and 1,3,6,8-tetra(4-carboxylphenyl)pyrene (TCPPY) as two building blocks through multiple π–π and hydrogen bond interactions. Owing to more efficient electron coupling effect, HOF-101 showed a 440-fold enhancement in ECL intensity compared with HOF-100, which indicated that establishing a tunable electron-coupled ECL system might light up a new way for investigating the intricate emission mechanism of HOFs. Like MOFs, HOFs can also be utilized as scaffolds to stabilize ECL luminophores to achieve signal-amplification. For instance, Shen et al. [152] prepared an ECL-active HOF by stabilizing abundant isoluminol molecules onto a self-assembled 2,4,6-tris(4-carboxyphenyl)-1,3,5-triazine (TATB) structure. TATB can catalyze the production of highly active oxygen-containing radicals ($OH^{\bullet}$ and $O_2{}^1$ radicals) for 23.4-fold signal amplification. Though the ECL studies on HOFs are still at the initial stage, it can be envisioned that more related investigations on ECL-active HOFs will be conducted in the future.

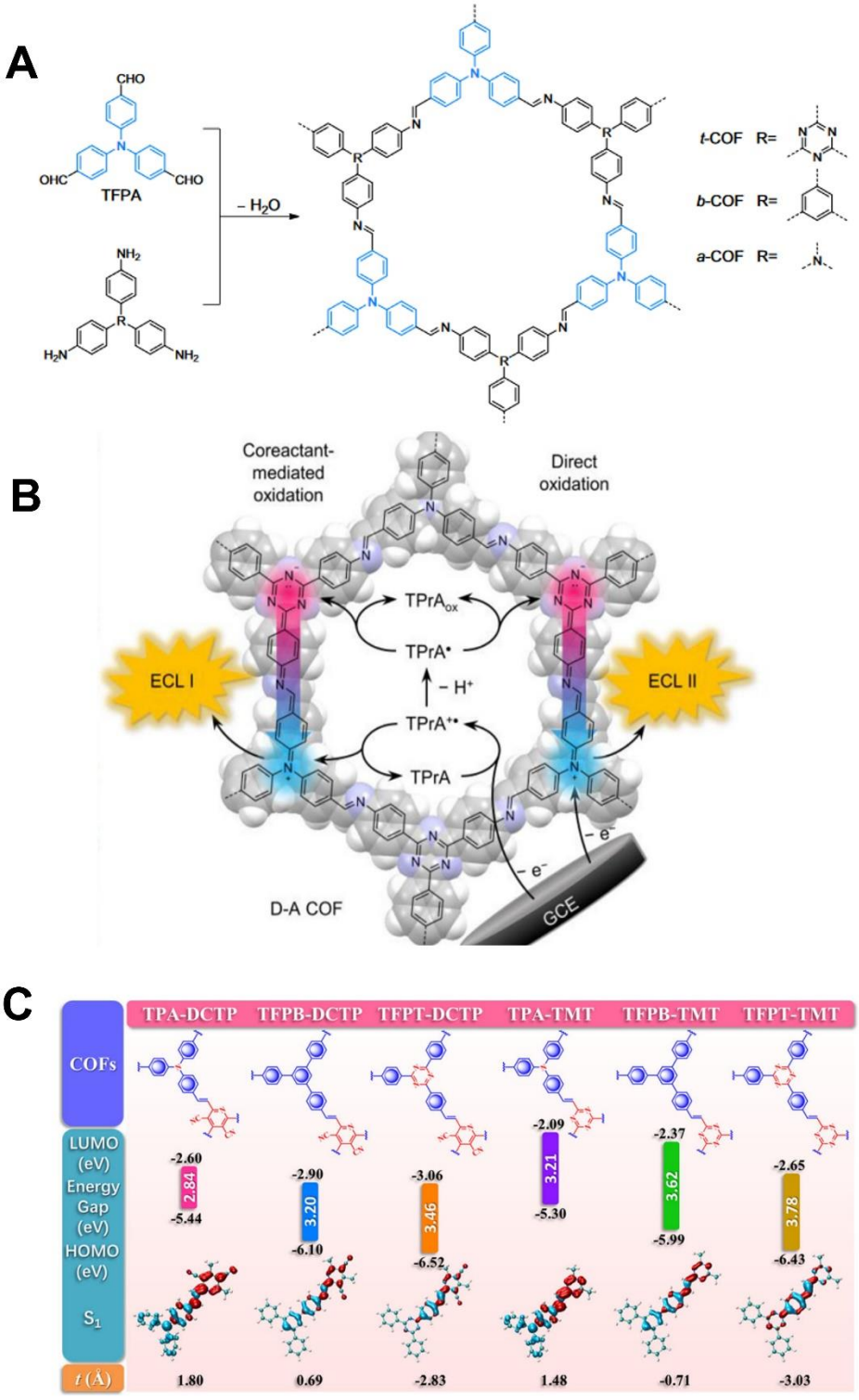


Figure 4. (**A**) Synthesis of three TFPA-based COFs and (**B**) schematic illustration of ECL mechanisms of COFs via the intrareticular charge transfer pathway. Reprinted with permission from Ref. [144], Copyright 2021 Springer Nature. (**C**) DFT calculations of COFs prepared by different organic building blocks with information on their corresponding HOMOs, LUMOs, calculated energy gaps, and *t* indexes. Reprinted with permission from Ref. [145], Copyright 2021 Springer Nature.

2.5. Polymer Dot-Based ECL Emitters

Since the first study of polymer dots (Pdots) by Bard et al. [153] in 2008, organic semiconductor Pdots as a kind of conjugated polymer nanoparticles (CNPs) have attracted

extensive attention for their excellent fluorescence behaviors, bright luminescence, desirable biocompatibility, and superb photostability [154]. Direct polymerization of low molecular weight monomers and post-polymerization of high molecular weight polymers have been recognized as two major synthetic procedures for Pdots [155]. Post-polymerization methods including microemulsion and reprecipitation are the most used techniques for Pdots preparation nowadays. Compared to those QDs-based ECL emitters, Pdots have superiorities of excellent biocompatibility and easy functionalization with versatile synthetic strategies, which making them a promising type of ECL emitter for biosensing and imaging [156]. Nevertheless, strong ECL emission for most Pdots can be only observed in organic solvents and their excitation potentials are high in the aqueous, thus their applications in aqueous bioassays are restricted [157]. To deal with this challenge, Dai et al. [158] fabricated hydrophilic Pdots by using triton X-100 as a capping regent to encapsulate poly[2-methoxy-5-(2-ethylhexyloxy)-1,4-phenylenevinylene] (MEH-PPV) via a reprecipitation method. The resulting Pdots performed good aqueous ECL emission via anodic, cathodic, and annihilation routes. As expanded research, electron-withdrawing cyano (CN) groups were attached to the MEH-PPV by Feng et al. [159] to act as block copolymers for preparing Pdots. The obtained CN-PPV Pdots performed significantly enhanced coreaction and annihilation ECL efficiencies in aqueous media. To date, some commercially available polyfluorene polymers such as poly (9,9-di-n-octylfluorenyl-2,7-diyl) (PFO) and poly[(9,9-dioctylindole-2,7-diyl)-co-(1,4-benzo-{2,1′-3}-thiadiazole)] (PFBT) have been used to prepare highly ECL-active Pdots for biosensing [160–162] and PFO Pdots [163,164]. Moreover, $Ru(bpy)_3^{2+}$, luminol, and other traditional ECL regents have also been employed as luminous units to fabricate ECL-active Pdots. For instance, 1354 $Ru(bpy)_3^{2+}$ molecules were averagely doped into a carboxylated conjugated polymer by Feng et al. [165] to obtain a highly ECL-active RuPdot for detecting single-nucleotide polymorphism. Then, a potential/color-resolved ECL bioassay was established by Wang et al. [166] using the luminol-doped polymer dots (L-Pdots) and diethylamine-coupled Pdots (N-Pdots) as dual ECL emitters for the simultaneous analysis of multiplex microRNAs. Considering the indispensable role that coreactant plays in ECL generation, it can be envisioned that high ECL efficiency can also be fulfilled by conjugating coreactant-active moieties with Pdots in shortened electron-transfer in one structure with less consumed radiative energy for ECL enhancement. More importantly, this strategy needs no exogenous coreactants which can be both eco-friendly and cost-effective. For the very first time, Wang et al. [167] fabricated a coreactant-free TEA-PFBT Pdot by attaching two tertiary amine (TEA) groups to the side chain of PFBT, which generated 132-fold boosted ECL emission through a dual intramolecular electron transition pathway without any exogenous coreactants, which emphasized the advances of fabricating coreactant-free ECL Pdots with extraordinary luminous efficiencies for bioassays.

Another interesting topic in this direction is the combination of conjugated polymer backbones with attractive AIEgens to prepare AIE-active Pdots [168,169]. As shown in Figure 5A, an AIE-active Pdot was synthesized by Wang et al. [168] through a Suzuki reaction between the boron ketoiminate (BKM) monomers and the AIEgen of TPE followed by nanoprecipitation of poly(styreneco-maleic anhydride) (PSMA). The obtained AIE-active Pdot was used as an ECL emitter which showed sensitive response to UO_2^{2+} in water environments. As shown in Figure 5B, Zhang et al. [169] incorporated AIE-active TPE moieties into the benzothiadiazole-based Pdots prepared by poly[4-(4-(2,2-bis(4-(octyloxy)phenyl)-1-phenylvinyl)phenyl)benzo-[c] [1,2,5] thiadiazole]. Benefiting from the AIECL property of TPE moieties, the prepared Pdots showed favorable sensing performances for nucleic acid detection. Notably, most of the reported methods for Pdots require nanoprecipitation of copolymers like PSMA with ECL-active moieties through weak noncovalent interactions. One should be concerned with the instability of the formed Pdots because of the possible desorption of those ECL-active moieties [170]. To further promote the advancement and application of Pdots-involved ECL sensing systems, covalent functionalization or some specific interactions with high affinities are expected to be introduced prior to or after the formation of Pdots, achieving better ECL stability for better sensing performances [171,172].

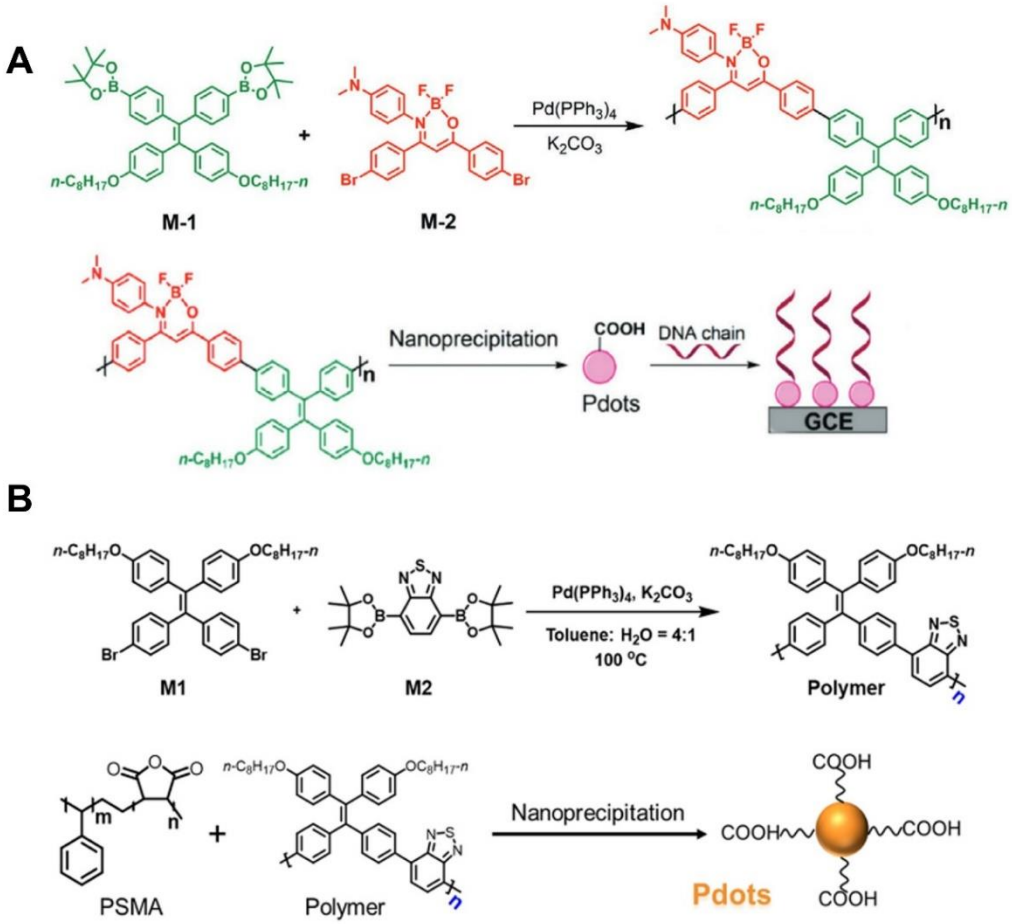


Figure 5. (**A**) Synthetic routes of AIE-active TPE-Pdots for electrode modification. Reprinted with permission from Ref. [168] Copyright 2020 Wiley. (**B**) Synthesis route of AIE-active iridium(III)-Pdots. Reprinted with permission from Ref. [169] Copyright 2021 American Chemical Society.

3. Application of ECL Emitters for the Analysis of Protein-Based Biomarkers

Biomarker, a kind of substance (gene, protein, polysaccharide, etc.) with valuable medical or biological significance, is generated from a normal physiological process or a biochemical pathway in the human body [34]. Pathologically related biomarker can give doctors insightful information about the health status of the body with minimal interference and less effort or warnings that a possible disease might be evolving, which is of great importance for patients to get the medical cure with efficient control of the disease in the early stages [173,174]. Biomarkers can be classified into imaging and non-imaging types. The former type is usually required in the X-rays or MIR imaging of diseases while the latter usually functions as a measurable indicator (protein, nucleic acid, small metabolite, cytogenetic, or cytokinetic factors) in body fluids or tissues that is closely relate to a certain disease. Among those types, protein-based biomarkers have been recognized as golden indicators for diagnosing various diseases in the early stages with trustful prognostic values [175–177]. As for the point-of-care detection of protein biomarkers with low abundance, great challenges are ahead due to the limited sensitivity of traditional assays, high background signals make it difficult to capture the accurate information of target protein rapidly in crude and complex samples without highly expensive and sophisticated instrumentations. ECL is now considered one of the most promising analytical techniques, owning superior sensitivity and ultralow background signals for biological applications with an ease of operation and rapid responses in real-time. With the aim of improving detection sensitivity and the reliability and accuracy in the diagnosis of protein biomarkers, a variety of promising and highly-efficient ECL nanomaterials were fabricated and employed as emitters of biosensors over the past decades.

3.1. Protein-Based Cancer Biomarkers

Protein biomarkers such as alpha fetoprotein (AFP), prostate-specific antigen (PSA), carcinoembryonic antigen (CEA), mucin 1 (MUC1), and cytokeratin 19 fragment (CYFRA 21-1), as recently studied by using advanced ECL emitters and biosensing strategies [173,175]. CEA as a broad-spectrum protein biomarker of malignant tumors is commonly related to potential pancreatic, colorectal, or breast cancer in human bodies [170]. To date, ECL biosensors have been developed as highly-sensitive tools for the clinical diagnosis of CEA-indicated cancers. For instance, the Zn^{2+}-doped Au NCs (Zn^{2+}-AIE-Au NCs) with AIE activity were prepared by Gao et al. [178] using mercaptopropionic acid as a capping regent. The Zn^{2+}-AIE-Au NCs as monochromatic (FWHM < 40 nm) emitters with high ECL efficiency were further integrated with the dual-stabilizer-capped $CuInS_2$@ZnS NCs to establish a spectrum-resolved ECL biosensor for multiplexing bioassay in real samples. In the assay, CEA was sensitively determined with an LOD of 0.3 pg/mL. Then, Zhang et al. [179] reported a band-edge effect-induced ECL immunosensor using the silica inverse opal photonic crystals (SIOPCs) for CEA incubation. The radiative transition probability was increased due to the formation of high density states at the band-edge in SIOPCs, which enhanced the photon extraction during propagation and achieved strong ECL outputs for CEA detection with an LOD of 0.032 pg/mL. To guarantee high accuracy, establishing a potential/wavelength- based ratiometric ECL assay is usually a preferred choice since it can provide self-calibration to decrease systematic errors and improve the detection reliability for CEA detection. As previously reported, Huang et al. [180] developed a dual-potential ECL immunoassay by using the highly ECL emissive luminol and CdS QDs as anodic and cathodic emitters, respectively. The assay showed ratio-metric ECL emission at −1.5 V and +0.3 V (vs. Ag/AgCl) using H_2O_2 as the coreactant which realized sensitive and accurate detection for CEA with an LOD of 0.62 pg/mL. With concern to the possible interferences between the two different ECL emitters in conventional ratiometric biosensors, Shang at al. [38] designed a potential-resolved ECL immunoassay by utilizing single emitters of luminol as the cathodic and the anodic emitter (−0.2 to 0.45 V, vs. Ag/AgCl). In this ratiometric assay, Pd NCs modified substrates could quench the anodic ECL (I_{anodic}) and amplify the anodic ECL ($I_{cathodic}$) of luminol −0.2 to 0.45 V, thus the detection results ($I_{cathodic}/I_{anodic}$) can be self-calibrated to endow the biosensor a stronger reliability for CEA detection with an ultralow LOD of 87.1 ag/mL. Obviously, ratiometric-typed ECL biosensors still hold great potential for the ultrasensitive detection of low-abundant protein biomarkers in complex samples in the future.

Recently, bipolar electrode (BPE) device as one of the most attractive electronic conductors based on bipolar electrochemistryhas attracted extensive scientific interest in the field of biosensing for protein biomarkers [181]. Li et al. [182] constructed a gold nanowire array-based BPE system using $Ru(bpy)_3{}^{2+}$-wrapped SiO_2 nanoparticles (Ru@SiO_2) as ECL emitters. The facile BPE sensing device realized sensitive detection of AFP expressed by the HepG2 cell surface with an LOD of 6.71 pg/cell. Meanwhile, Yu et al. [183] developed a near-infrared ECL immunoassay by using the biocompatible and environmentally friendly methionine-stabilized Au NCs as ECL emitters for AFP detection. The assay performed a good selectivity for AFP in complex samples with an ultralow LOD of 1 fg/mL, which was much lower than those reported ECL biosensors.

PSA, as a single-chain glycoprotein, is regarded as the most representative indicator for the early diagnosis of prostate cancer, the second most fatal cancer for men [184]. Qin et al. [185] developed a dual-quenching ECL immunoassay for PSA detection on a solid-state platform fabricated by the modification of an AIE-active layer of 6-aza-2-thiothymine capped Au NCs (ATT-Au NCs). The ECL emission of ATT-Au NCs can be regulated by the CeO_2-PEI@Ag probe via resonance energy transfer, thus achieving a sensitive detection of PSA with an LOD of 2.2 fg/mL lower than previously reported works. Wang et al. [184] designed a label-free PSA aptasensor based on the luminol-functionalized molecularly imprinted polymers (MIP) of electropolymerized dopamine (DA) film. Relying on the specific interaction of PSA with aptamer-covered imprinted cavities, the aptasensor

exhibited gradually decreased ECL signals along with increased PSA concentration in the linear range of 5 pg/mL–50 ng/mL, achieving a low LOD of 3.0 pg/mL with acceptable stability and reproducibility. Considering the limited sensitivity of the label-free sensing format, as a following work, Wang et al. [40] further developed an ECL quenching strategy by using the carboxylated graphitic carbon nitride nanosheet as the donor and Ru@SiO_2 as the acceptor. Through the efficient electron-transfer mediated quenching mechanism, high sensitivity was achieved for PSA determination along with a rather low LOD of 1.2 fg/mL. In addition, an efficient ECL-RET aptasensor for PSA detection was constructed by Zhao et al. [186] using the Cys-$[Ru(dcbpy)_3]^{2+}$ as ECL emitters whose emission could be flexibly quenched by the ZnS QDs loaded mesoporous silica nanocontainers (ZnS@SiO_2) via a controlled releasing strategy (Figure 6). Due to the efficient ECL-RET between Cys-$[Ru(dcbpy)_3]^{2+}$ and ZnS@SiO_2, the detection sensitivity and accuracy for PSA detection were desirable, showing a low LOD of 1.01 fg/mL. Besides, other promising highly ECL-emissive NCs such as dual-stabilizer-capped InP/ZnS NCs and Ag-Ga-In-S NCs have also been fabricated as ECL emitters for PSA detection by Zou's group [77,187], which highly indicated the promising application potential of multinary NCs in the clinical diagnosis of protein biomarkers.

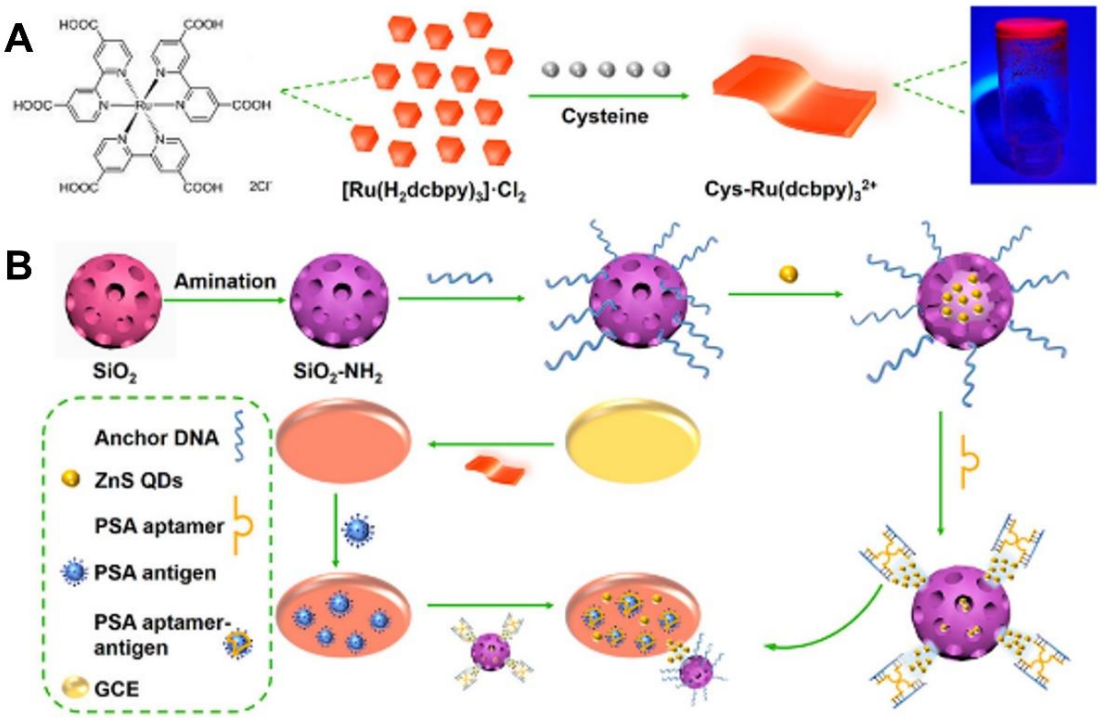


Figure 6. (**A**) Preparation procedures of Cys-$[Ru(dcbpy)_3]^{2+}$ and ZnS@SiO_2-ssDNA/apta. (**B**) Fabrication process of constructed aptasensor for PSA detection. Reprinted with permission from Ref. [186], Copyright 2023 American Chemical Society.

Lung cancers, including small cell lung cancer (SCLC) and non-small cell lung cancer (NSCLC), have become the primary worldwide cause of cancer mortality with the fastest growing incidence rate nowadays. Biomarkers for lung cancer including CEA, CYFRA 21-1 squamous cell carcinoma antigen (SCCA), and neuron-specific enolase (NSE) have exhibited tremendous potential as trustful indicators for lung cancer diagnosis in early stages [170]. To date, various ECL biosensing systems have been established for NSE detection [114,188–190]. For example, Dong et al. [114] prepared a $Ru(bpy)_3^{2+}$ functionalized Zr-MOF (Ru-MOF-5) as a dual-signal ratiometric ECL platform, achieving efficient dual-potential ECL emission for detecting NSE lower to 41 fg/mL along with self-calibrated detection accuracy. Furthermore, Han et al. [190] developed a sensitive NSE immunoassay by utilizing the nitrogen-doped CQDs (N-CQDs) as ECL emitters. The sensitivity of

this assay was enhanced by introducing the coreaction accelerator of molybdenum sulfide/ferric oxide (MoS_2@Fe_2O_3) nanocomposites as an incubation substrate, achieving an ultralow LOD of 6.30 fg/mL with favorable performance. CYFRA 21-1 is a trustful protein biomarker for non-small cell lung cancer (NSCLC) which holds great reference value in the early stages of NSCLC. Recently, great efforts have been devoted into developing CYFRA 21-1 immunoassays with higher sensitivity and accuracy [191–193]. For example, Yang et al. [193] fabricated an AIE-active biocompatible ECL emitter by encapsulating *fac*-tris(2-phenylpyridine)iridium(III) complexes [Ir(ppy)$_3$] into an apoferritin (apoFt) cavity for CYRFA 21-1 detection based on a conductive and electroactive substrate of Fe_2N and Au NP-loaded rGO (Fe_2N/rGO/Au). Li et al. [194] proposed a BPE-assisted ECL immunoassay based on the glucose oxidase and horseradish peroxidase loaded ZIF-67@CaO_2 composites. ZIF-67@CaO_2 can in situ produce coreactants of O_2 and H_2O_2 to promote ECL reaction of luminol to realize the sensitive detection of CYFRA 21-1 with favorable performance.

3.2. Protein-Based Non-Cancer Biomarkers

Instead of focusing on cancer biomarkers, ECL biosensing systems have been developed for various protein biomarkers of other major diseases such as Alzheimer's disease (AD), cardiovascular diseases, sepsis, and so on [108,136,195–197]. AD has become a worldwide brain disease that threatened the physical health of the aged [197]. How to protect them from the AD attack and obtain timely medical treatment in the early stage is of great importance. Amyloid-β protein (A$\beta_{1–42}$) was recognized as the most critical and predictive protein biomarker for diagnosing AD. ECL-based biosensing strategies have been developed for the specific and sensitive analysis of A$\beta_{1–42}$ [27,108,198,199]. Recently, Qin et al. [200] proposed dual-wavelength ratiometric ECL immunoassays for A$\beta_{1–42}$ analysis based on twoECL emitters including Ru@TiO_2@Au (620 nm) and AuNPs-modified g-C_3N_4 (460 nm) with different emission wavelengths. By virtue of the ECL-RET between these two emitters, sensitive detection of A$\beta_{1–42}$ was achieved with an ultralow LOD of 2.6 fg/mL in cerebrospinal fluid. Also, Tan et al. [198] developed an advanced ECL aptasensing system by combining affinity screening of aptamers and size screening of silica nanochannels. The sensing mechanism was operated by the steric hindering formed by the specific interaction of A$\beta_{1–42}$ on the aptamer in arrayed nanochannels, which blocked the mass transport of luminol and led to ECL reduction in corresponding to the A$\beta_{1–42}$ concentration. Recently, Alzheimer-associated neuronal thread protein (AD7c-NTP) was found in the CSF, blood, and urine of AD patients and can be regarded as a new and trustful biomarker for AD diagnosis [201]. However, only enzyme-linked immunosorbent assays (ELISA) were used for AD7c-NTP detection. To obtain higher sensitivity than ELISA, the superior ECL technique was more suitable for ultra-trace analysis of AD7c-NTP. Liang et al. [202] recently constructed a dry chemistry-based BPE device for the ECL assay of AD7c-NTP. This device was composed of a screen-printed fiber chip filled with a Ru(II)-poly-L-lysine complex for immunoreaction where self-enhanced ECL detection can be completed in 6 min with an LOD of 0.15 pg/mL in human urine samples.

Heart diseases including acute myocardial infarction (AMI) and heart failure (HF) have comparable mortality rates to that of cancers and have become the most concerning class of disease that severely threatens the body health of human beings all around the world [203]. C-reactive protein (CRP) and cardiac troponin I (cTnI) are two common protein biomarkers for AMI and cardiovascular diseases [204]. Yang et al. [205] synthesized a series of novel multicolor iridium(III) complexes, among which the adap-based Ir(III) complexes exhibited a good binding affinity with β-cyclodextrin (β-CD) due to the strong hydrophobic interaction and acted as ECL emitters for aqueous-phase detection of CRP with an LOD of 72 pg/mL. Hong et al. [206] developed an ECL combined lateral flow immunoassay (ECL-LFI) which was suitable for full-range analysis of physiological CRP levels. This assay involved the usage of Ru(bpy)$_3^{2+}$-labeled AuNPs as CRP probes which plays an important role in the test line of the strip to achieve a sensitive and rapid read-out with a low LOD of 4.6 pg/mL in the clinical diagnosis of AMI. Guo et al. [207] designed

an ECL emitter-free and disposable biosensor based on the quenched cathodic signal of porous TiO_2 microspheres by the ferrocene labeled Y-shaped probes. This efficient signal "off-on" assay showed good linearity in 100 fg/mL–100 ng/mL with a low LOD of 30.1 fg/mL for cTnI detection in human serum. Heart failure, as the result of the systolic or diastolic dysfunction of the heart, is usually regarded as the terminal stage of many cardiovascular diseases [196]. *N*-terminal pro-brain natriuretic peptide (NT-proBNP) has been established as a key biomarker which owns prognostic importance for heart failure and other cardiovascular diseases [170]. Luo et al. [195] proposed a simple and sensitive ECL-sensing device by using luminol functionalized AuNPs/ZIF-67 as an ECL emitter which can achieve sensitive NT-proBNP detection lower to 0.74 pg/mL with good specificity and stability. Ji et al. [208] designed a dual-signal ECL immunoassay by using the $Ru(bpy)_3^{2+}$@HKUST-1 as anodic ECL emitters and $Ce_2Sn_2O_7$ nanocubes as the cathodic emitters in which the detection accuracy for NT-proBNP was well improved, benefiting from the self-calibration of anodic and cathodic ECL responses (Figure 7).

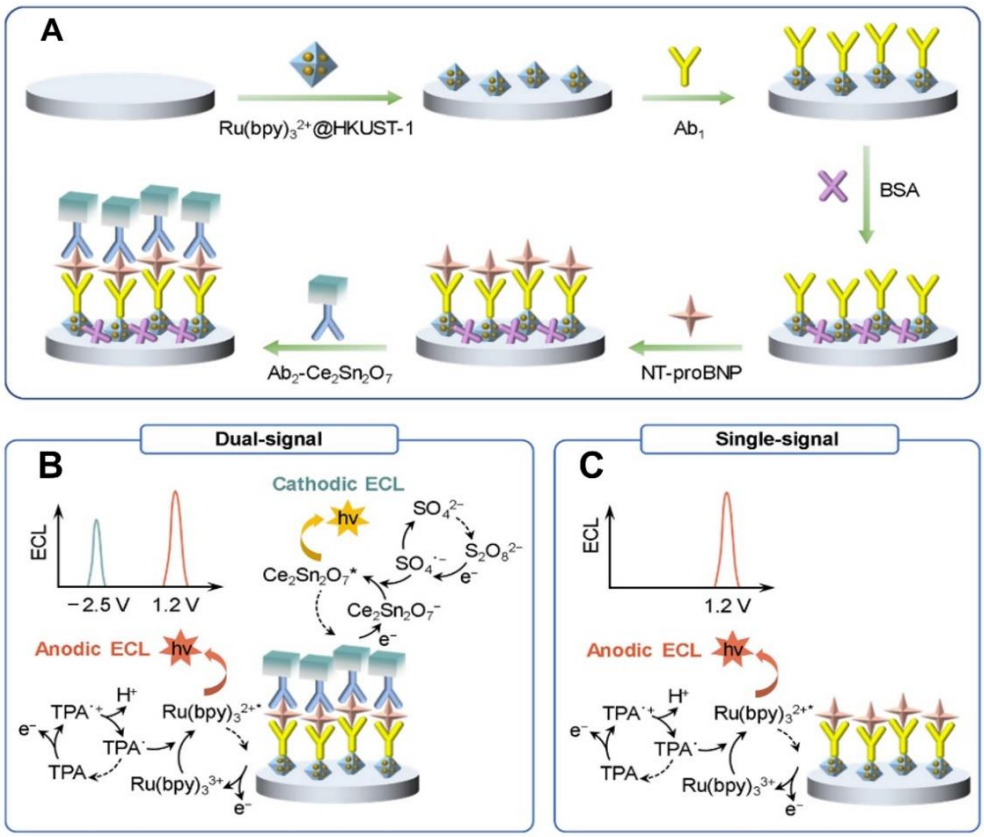


Figure 7. (**A**) Schematic illustration of a dual-signal ECL immunosensor for NT-proBNP detection. (**B**) Dual-signal and (**C**) single-signal ECL mechanisms. Reprinted with permission from Ref. [208] Copyright 2023 Royal Society of Chemistry.

Sepsis is a systemic response to infection most often caused by bacteria and results in life-threatening inflammation throughout the body. Procalcitonin (PCT) secreted by thyroid C cells has shown a strong correlation with the severity of sepsis, which is recognized as a representative biomarker in the early diagnosis of sepsis. Xu et al. [209] developed a quenching-typed ECL immunosensor based on ferrocene carboxylic acid (Fca) quenching the ECL of the $Ru(bpy)_3^{2+}$ and TPrA co-encapsulated ECL SiO_2 NPs. In this assay, good sensitivity for PCT detection was achieved by an electron-transfer mediated quenching mechanism which contributed to the low LOD of 0.85 pg/mL. Instead of the quenching method, ECL-RET was also recognized as a highly sensitive technique for PCT detection. Song et al. [210] designed an ECL-RET immunosensor by employing the carbon nanotubes

(CNT) and Au-functionalized graphitic carbon nitride (g-C_3N_4–CNT@Au) as the ECL donor and CuO nanospheres-polydopamine (PDA) layer (CuO@PDA) as the receptor, respectively. High RET efficiency from g-C_3N_4–CNT@Au to CuO@PDA was occurred for sensitive detection of PCT lower to 25.7 fg/mL in human serum. In addition, Wang et al. [211] prepared a dual-emitting ECL immunosensor by employing MnO_2 nanoflowers (NFs) and ZnS QDs as dual ECL emitters with $S_2O_8^{2-}$ as the coreactant which exhibited a good linearity in the range of 0.1 pg/mL to 100 ng/mL with an LOD of 0.033 pg/mL for PCT detection in serum. Most recently, Song et al. [212] designed a ternary ECL sensing system using lipoic acid (LA) capped Ag NCs as cathodic ECL emitters in $S_2O_8^{2-}$ containing electrolytes. In this assay, ligand-to-metal charge transfer between LA and Ag NCs induced ideal ECL emission which endowed the PCT immunosensor a low LOD of 3.56 fg/mL.

3.3. ECL Imaging

In recent years, ECLM as a fascinating optical microscopy technique has gained dramatically increased scientific interest in spatiotemporally resolved imaging of single NP or cell indicated by some specifically triggered ECL processes at the electrode surface [96,213]. Compared with traditional optical microscopy, ECLM owns superior features includingspatiotemporally controlled high resolution and high throughput r bioimaging of various membrane molecules at single-cell level [5,214]. More importantly, ECLM needs no extrinsic illumination source, which can eliminate those potential local photothermal effects and background noises for high-quality imaging [215]. Uniquely from serum analysis, specific visualization of protein biomarkers on cell membranes provides paramount information for elucidating molecular mechanisms in a wide variety of diseases [216]. To date, ECLM protocols have been gradually established to evaluate expression levels of protein biomarkers on cell membranes. Lu et al. [217] designed an efficient ECL nanoreactor for direct visualization of single membrane epithelial cell-adhesion molecule (EpCAM) proteins on heterogeneous MCF-7 cells by employing the $Ru(bpy)_3^{2+}$-loaded nanoporous zeolite nanoparticles (Ru@zeolite) as imaging probes (Figure 8). In the assay, nanoconfinement-enhanced ECL emission of $Ru(bpy)_3^{2+}$-TPrA was triggered in every single nanoreactor, which was conducive to achieving high-resolution ECL imaging of membranal biomarkers including AFP, PSA, and CEA. Liu et al. [10] proposed an ECL imaging strategy by using $Ru(bpy)_3^{2+}$-doped silica/Au NPs (RuDSNs/AuNPs) as probeswhich could create surface-confinement-controlled ECL enhancement for realizing single-molecule imaging of a protein biomarker of cytokeratin 19 at the electrode surface and cellular membrane. Liu et al. [218] developed a potential-resolved ECL imaging method for the diagnosis of apoptosis at the single-cell level. In the method, the epidermal growth factor receptor and phosphatidylserine were visualized on the surfaces of normal and cancer cell samples using g-C_3N_4 and Au@L012 as dual imaging probes. The assay not only offered a reliable imaging technique for the detection of various membrane biomarkers at the single-cell level, but also contributed to the guidance of rational drug applications for medical treatments. As well known, the addition of exogenous coreactants such as H_2O_2 or TPrA might induce potential cytotoxicity, thus making it quite urgent to design coreactant-free ECL emitters for cell imaging [219]. Wang et al. [167] designed coreactant-embedded polymer dots (TEA-Pdots) for in situ ECL imaging of single membrane protein without exogenous coreactant via an efficient intramolecular electron transfer mechanism. In addition to fabricating coreactant-embedded ECL emitters, developing biocompatible ECL coreactants is another doable and promising option. Chen et al. [219] prepared a guanine-rich DNA-aptamer complex that can not only function as the biocompatible coreactant for $Ru(bpy)_3^{2+}$ emission via a catalytic pathway but also specifically interact with overexpressed CEA on cell membranes for ECL imaging. Moreover, some it has been proved that high resolution for ECL imaging of membrane proteins can also be achieved without the direct utilization highly emissive probes. The pioneering work was reported by Zhang et al. [220]. They established capacitance-based ECL microscopy for the high-resolution imaging of low abundance CEA on the cellular plasma membrane without using any imaging probes. The

system was dominated by the principle of locally dropped capacitance upon the binding of target proteins to the surface or cellular membrane without using any ECL emitters which opened up a brand-new avenue for efficient ECL bioimaging of membrane protein biomarkers in a label-free manner.

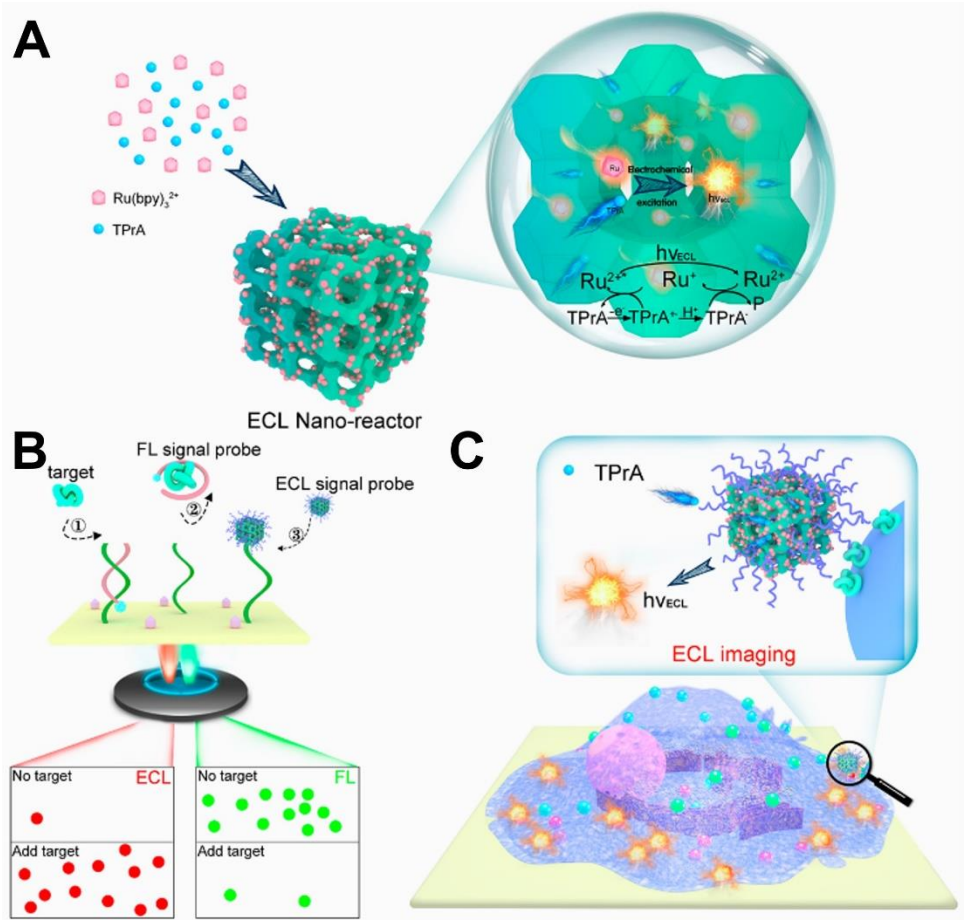


Figure 8. (**A**) Scheme for the nanoconfinement-enhanced ECL reaction at single nanoreactors. (**B**) Dual-signal (FL and ECL) imaging procedures ①–③ for individual protein analysis. (**C**) ECL imaging of a single protein on the cell membrane. Reprinted with permission from Ref. [217] Copyright 2023 American Chemical Society.

Despite that some advanced progress has been achieved in ECL imaging of protein biomarkers at the single-cell level, ECLM can also be employed as a powerful technique for other biological applications such as photodynamic therapy (PDT) and cell-adhesion visualizations. For instance, Chen et al. [221] established an ECL-driven PDT system which was dominated by the ECL-RET mechanism using $Ru(bpy)_3^{2+}$ as the donor and photo-sensitizer of chlorin e6 (Ce 6) as the acceptor. The mechanism revealed that the ECL emission of $Ru(bpy)_3^{2+}$ could sensitize the surrounding O_2 to produce ROSs to kill cancer cells. Moreover, ECLM has also been applied to investigate the cell matrix adhesion process in a visual view [222,223]. Ding et al. [222] reported a label-free strategy to image the cell-matrix adhesion of living cells on a silica nanochannel membrane-based electrode at the single-cell level. The ECL reaction was triggered between freely diffused $Ru(bpy)_3^{2+}$ and coreactants, which showed a direct visualization of different adhesion sites of living cells, thus offering more precise information for imaging cellular orientations during the collective migrations in a label-free manner. Moreover, Ding et al. [223] proposed a surface-sensitive ECLM imaging method to evaluate possible impacts of different chemically modified substrates on cell adhesions. As observed from the statistical analysis of spatial distribution, area, and strength of cell adhesion, Arg–Gly–Asp (RGD) modified electrodes

can mediate robust cell matrix interactions. This work showcased that ECLM can be a qualified tool to analyze other cell behaviors during cancer metastasis on different microenvironments with high sensitivity and resolution.

4. Summary and Perspectives

Applying a highly-efficient emitter is the core of an ECL analytical system to obtain the high sensitivity and accuracy for target detection. Along with the interdisciplinary integration of electrochemistry, spectroscopy, and nanotechnology, various nanomaterial-based ECL emitters were developed and injected numerous vitalities into ECL bioassays with significantly improved analytical performances. In this review, we mainly focused on the recently reported fabrication of some attractive ECL emitters including QDs, MeNCs, MOFs, COFs/HOFs, and Pdots and their advances in sensitive ECL sensing and spatiotemporally resolved imaging of protein-based biomarkers. Through decent designation, high ECL efficiencies can be easily achieved among these ECL emitters. As for the preparation methods, QDs, MOFs, COFs, HOFs, and Pdots often require complicated organic synthetic procedures to obtain needed ligands or hydrothermal processes with high temperatures and pressures. Water stability issues for QDs, MeNCs, and MOFs should also be carefully concerned for aqueous application. Those nanosized QDs, MeNCs, and Pdots possess greater potential for high-resolution bioimaging than MOFs and COFs/ HOFs with larger sizes. Instead, MOFs, COFs/HOFs with large specific areas and electrochemical activity can be flexibly employed to develop promising ECL solid-sate devices for point-of-care application. In order to aim for higher-level advancements, opportunities and challenges are considered and addressed in this section to obtain a clear understanding of development trends in the future.

Obtaining extraordinary ECL efficiency via a newly established excited-state generation mechanism is becoming one of the most promising directions for exploiting high-quality ECL emitters. As for those above-mentioned QDs, MeNCs, MOFs, COFs, HOFs, and Pdots, most of their triplet excitons were consumed via nonradiative decay; only ~25% of the generated singlet excitons were decayed radiatively with a low ECL efficiency. Paving a new way to promote the utilization rate of triplet excitons with a proper theoretical model is urgently demanded. Some advanced efforts in the antenna effect, thermal activation of delayed luminescence, and triplet–triplet annihilation on this topic have been gradually exploited with significantly increased ECL efficiencies which injected new insights of the investigations on new ECL mechanisms.

Considering that most of the ECL bioassays are developed following the sandwich-typed format, efficient bioactivity maintenance of biomolecules in this format is of great importance. Interferences from the sensing substrate, probe, and electrolytes including pH and ionic strength toward the bioactivity of used biorecognition molecules like antibodies or aptamers should be carefully evaluated to guarantee the accuracy and practicability of immunosensors. Therefore, constructing more biocompatible interfaces on ECL emitters and substrates with vigorous and anti-interferent biorecognition molecules is becoming another attracting direction in which more endeavors are suggested to be devoted to establishing more robust specific interactions to capture the detection targets effectively. In this way, we believe that the developed ECL biosensor will perform better specificity, reproducibility, and reliability for practical applications.

In addition, a variety of advanced imaging methods combined with promising ECL emitters were displayed for membrane protein sensing at a single-cell level. No one can deny that the ECL imaging technique combined with immunoassays for the high-throughput detection of membrane biomarkers will become one of the most attractive microscopic branches in the future. Though some grounding breakthroughs have been achieved, no one can deny that the conventional $Ru(bpy)_3^{2+}$-TPrA system is mostly used for ECL imaging. To obtain stronger intensity, $Ru(bpy)_3^{2+}$ molecules are usually stabilized in a biocompatible carrier like SiO_2 NPs to act as imaging probe while the cell-incubated substrate is still immersed into electrolytes containing TPrA whose biotoxicity on cell

viability is inevitable. Obviously, designing biocompatible coreactant is a doable idea to embrace the challenge. Also, preparing self-enhanced ECL emitters by implanting or modifying the coreactant-active moieties with luminophores can be regarded as an ideal alternative which needs no exogenous coreactant to directly contact the live cells. It can be envisioned that coreactant-free sensing strategies will present great application potential toward the development of eco-friendly ECL immunoassays or bioimaging in the future.

To summarize, the fabrication and application of novel and highly-efficient ECL emitters for biosensing and imaging are still incredibly exciting. They enriched the resources of synthetic routes for different kinds of nanomaterials, wide applications for various disease-related protein biomarkers, and advanced imaging techniques with high spatial-temporal resolution. ECL biosensors with advantages of being miniaturized, portable, easy to integrate with other devices, are still highly encouraged to create a bridge between lab research and commercialization. We believe that the remarkable ECL technique will open more scientific possibilities for the establishment of sophisticated mechanism models, achieving widely expanded applications in biosensing and imaging with favorable social and economic benefits.

Author Contributions: Writing—original draft preparation, L.Y.; Writing—review and editing, supervision, funding acquisition, J.L. All authors have read and agreed to the published version of the manuscript.

Funding: This work was financially supported by the National Key Research and Development Program of China (No. 2021YFA1200104), New Cornerstone Science Foundation, National Natural Science Foundation of China (No. 22027807, No. 22034004), Strategic Priority Research Program of Chinese Academy of Sciences (No. XDB36000000), Special support from China Postdoctoral Science Foundation (2022TQ0171), and Tsinghua-Vanke Special Fund for Public Health and Health Discipline Development (No. 2022Z82WKJ003).

Institutional Review Board Statement: Not applicable.

Informed Consent Statement: Not applicable.

Data Availability Statement: Not applicable.

Conflicts of Interest: The authors declare no competing financial interest.

References

1. Hu, L.; Xu, G. Applications and trends in electrochemiluminescence. *Chem. Soc. Rev.* **2010**, *39*, 3275–3304. [CrossRef] [PubMed]
2. Yang, X.; Hang, J.; Qu, W.; Wang, Y.; Wang, L.; Zhou, P.; Ding, H.; Su, B.; Lei, J.; Guo, W.; et al. Gold Microbeads Enabled Proximity Electrochemiluminescence for Highly Sensitive and Size-Encoded Multiplex Immunoassays. *J. Am. Chem. Soc.* **2023**, *145*, 16026–16036. [CrossRef]
3. Wang, Y.; Ding, J.; Zhou, P.; Liu, J.; Qiao, Z.; Yu, K.; Jiang, J.; Su, B. Electrochemiluminescence Distance and Reactivity of Coreactants Determine the Sensitivity of Bead-Based Immunoassays. *Angew. Chem. Int. Ed.* **2023**, *62*, e202216525. [CrossRef]
4. Miao, W. Electrogenerated Chemiluminescence and Its Biorelated Applications. *Chem. Rev.* **2008**, *108*, 2506–2553. [CrossRef]
5. Voci, S.; Goudeau, B.; Valenti, G.; Lesch, A.; Jović, M.; Rapino, S.; Paolucci, F.; Arbault, S.; Sojic, N. Surface-Confined Electrochemiluminescence Microscopy of Cell Membranes. *J. Am. Chem. Soc.* **2018**, *140*, 14753–14760. [CrossRef] [PubMed]
6. Visco, R.E.; Chandross, E.A. Electroluminescence in Solutions of Aromatic Hydrocarbons. *J. Am. Chem. Soc.* **1964**, *86*, 5350–5351. [CrossRef]
7. Han, Q.; Wang, C.; Liu, P.; Zhang, G.; Song, L.; Fu, Y. Three kinds of porphyrin dots as near-infrared electrochemiluminescence luminophores: Facile synthesis and biosensing. *Chem. Eng. J.* **2021**, *421*, 129761. [CrossRef]
8. Nasiri Khonsari, Y.; Sun, S. Recent trends in electrochemiluminescence aptasensors and their applications. *Chem. Commun.* **2017**, *53*, 9042–9054. [CrossRef]
9. Li, Z.; Huang, X.; Liu, H.; Luo, F.; Qiu, B.; Lin, Z.; Chen, H. Electrochemiluminescence Biosensor for Hyaluronidase Based on the Adjustable Electrostatic Interaction between the Surface-Charge-Controllable Nanoparticles and Negatively Charged Electrode. *ACS Sens.* **2022**, *7*, 2012–2019. [CrossRef]
10. Liu, Y.; Zhang, H.; Li, B.; Liu, J.; Jiang, D.; Liu, B.; Sojic, N. Single Biomolecule Imaging by Electrochemiluminescence. *J. Am. Chem. Soc.* **2021**, *143*, 17910–17914. [CrossRef]
11. Yang, X.; Yuan, R.; Chai, Y.; Zhuo, Y.; Mao, L.; Yuan, S. $Ru(bpy)_3^{2+}$-doped silica nanoparticles labeling for a sandwich-type electrochemiluminescence immunosensor. *Biosens. Bioelectron.* **2010**, *25*, 1851–1855. [CrossRef]

12. Dong, Y.-P.; Chen, G.; Zhou, Y.; Zhu, J.-J. Electrochemiluminescent Sensing for Caspase-3 Activity Based on $Ru(bpy)_3^{2+}$-Doped Silica Nanoprobe. *Anal. Chem.* **2016**, *88*, 1922–1929. [CrossRef] [PubMed]
13. Valenti, G.; Rampazzo, E.; Bonacchi, S.; Petrizza, L.; Marcaccio, M.; Montalti, M.; Prodi, L.; Paolucci, F. Variable Doping Induces Mechanism Swapping in Electrogenerated Chemiluminescence of $Ru(bpy)_3^{2+}$ Core–Shell Silica Nanoparticles. *J. Am. Chem. Soc.* **2016**, *138*, 15935–15942. [CrossRef] [PubMed]
14. Yue, Q.; Li, X.; Fang, J.; Li, M.; Zhang, J.; Zhao, G.; Cao, W.; Wei, Q. Oxygen Free Radical Scavenger PtPd@PDA as a Dual-Mode Quencher of Electrochemiluminescence Immunosensor for the Detection of AFB1. *Anal. Chem.* **2022**, *94*, 11476–11482. [CrossRef] [PubMed]
15. Huang, J.; Xiang, Y.; Li, J.; Kong, Q.; Zhai, H.; Xu, R.; Yang, F.; Sun, X.; Guo, Y. A novel electrochemiluminescence aptasensor based on copper-gold bimetallic nanoparticles and its applications. *Biosens. Bioelectron.* **2021**, *194*, 113601. [CrossRef]
16. Lin, Y.; Cao, J.; Li, X.; Zhang, X.; Zhang, J.; Lin, Z. A novel molecularly imprinted electrochemiluminescence sensor based on a $Ru(bpy)_3^{2+}$/MWCNTs/nano-TiO_2-Nafion electrode for the detection of bisphenol A. *Anal. Methods* **2016**, *8*, 7445–7452. [CrossRef]
17. Ju, J.; Ding, Q.; Xie, J.; Li, G. Label-free electrochemiluminescence immunosensor for mucoprotein 1 using a graphene oxide-$Ru(Bpy)_3^{2+}$-polyaniline nanocomposite. *Anal. Lett.* **2023**, 1–12. [CrossRef]
18. Lin, J.; Wu, H.; Lu, L.; Sun, Z.; Zhang, Y.; Dang, F.; Qian, L. Porous graphene containing immobilized Ru(II) tris-bipyridyl for use in electrochemiluminescence sensing of tripropylamine. *Microchim. Acta* **2016**, *183*, 1211–1217. [CrossRef]
19. Yang, W.; Zhang, G.; Ni, J.; Wang, Q.; Lin, Z. From signal amplification to restrained background: Magnetic graphene oxide assisted homogeneous electrochemiluminescence aptasensor for highly sensitive detection of okadaic acid. *Sens. Actuators B Chem.* **2021**, *327*, 128872. [CrossRef]
20. Gao, W.; Chen, Y.; Xi, J.; Zhang, A.; Chen, Y.; Lu, F.; Chen, Z. A novel electrochemiluminescence sensor based on $Ru(bpy)_3^{2+}$ immobilized by graphene on glassy carbon electrode surface via in situ wet-chemical reaction. *Sens. Actuators B Chem.* **2012**, *171–172*, 1159–1165. [CrossRef]
21. Yao, B.; Zhang, J.; Fan, Z.; Ding, Y.; Zhou, B.; Yang, R.; Zhao, J.; Zhang, K. Rational Engineering of the DNA Walker Amplification Strategy by Using a Au@Ti_3C_2@PEI-$Ru(dcbpy)_3^{2+}$ Nanocomposite Biosensor for Detection of the SARS-CoV-2 RdRp Gene. *ACS Appl. Mater. Interfaces* **2021**, *13*, 19816–19824. [CrossRef]
22. Xing, H.; Xia, H.; Fan, Y.; Xue, Y.; Peng, C.; Ren, J.; Li, J.; Wang, E. A Solid-State Electrochemiluminescence Sensor Based on Novel Two-Dimensional Ti_3C_2 MXene. *ChemElectroChem* **2021**, *8*, 1858–1863. [CrossRef]
23. Fang, Y.; Yang, X.; Chen, T.; Xu, G.; Liu, M.; Liu, J.; Xu, Y. Two-dimensional titanium carbide (MXene)-based solid-state electrochemiluminescent sensor for label-free single-nucleotide mismatch discrimination in human urine. *Sens. Actuators B Chem.* **2018**, *263*, 400–407. [CrossRef]
24. Wang, Y.; Shan, D.; Wu, G.; Wang, H.; Ru, F.; Zhang, X.; Li, L.; Qian, Y.; Lu, X. A novel "dual-potential" ratiometric electrochemiluminescence DNA sensor based on enhancing and quenching effect by G-quadruplex/hemin and Au-Luminol bifunctional nanoparticles. *Biosens. Bioelectron.* **2018**, *106*, 64–70. [CrossRef] [PubMed]
25. Gao, X.; Ren, X.; Ai, Y.; Li, M.; Zhang, B.; Zou, G. Luminophore-Surface-Engineering-Enabled Low-Triggering-Potential and Coreactant-Free Electrochemiluminescence for Protein Determination. *Anal. Chem.* **2023**, *95*, 6948–6954. [CrossRef] [PubMed]
26. He, Y.; Du, J.; Luo, J.; Chen, S.; Yuan, R. Coreactant-free electrochemiluminescence biosensor for the determination of organophosphorus pesticides. *Biosens. Bioelectron.* **2020**, *150*, 111898. [CrossRef]
27. Xie, J.; Yang, G.; Tan, X.; Yuan, R.; Chen, S. Coreactant-free electrochemiluminescence of polyfluorene nanoparticle coupling double quencher for β-amyloid$_{1\text{-}42}$ detection. *Talanta* **2023**, *258*, 124398. [CrossRef]
28. Song, X.; Zhao, L.; Luo, C.; Ren, X.; Wang, X.; Yang, L.; Wei, Q. Bioactivity-protective electrochemiluminescence sensor using CeO_2/Co_4N heterostructures as highly effective coreaction accelerators for ultrasensitive immunodetection. *Sens. Actuators B Chem.* **2022**, *355*, 131158. [CrossRef]
29. Wu, F.-F.; Zhou, Y.; Zhang, H.; Yuan, R.; Chai, Y.-Q. Electrochemiluminescence Peptide-Based Biosensor with Hetero-Nanostructures as Coreaction Accelerator for the Ultrasensitive Determination of Tryptase. *Anal. Chem.* **2018**, *90*, 2263–2270. [CrossRef]
30. Yang, G.; Zhang, Y.; Zhao, J.; He, Y.; Yuan, R.; Chen, S. Dual-emitting Iridium nanorods combining dual-regulating coreaction accelerator Ag nanoparticles for electrochemiluminescence ratio determination of amyloid-β oligomers. *Biosens. Bioelectron.* **2022**, *216*, 114629. [CrossRef]
31. Ma, C.; Cao, Y.; Gou, X.; Zhu, J.-J. Recent Progress in Electrochemiluminescence Sensing and Imaging. *Anal. Chem.* **2020**, *92*, 431–454. [CrossRef]
32. Husain, R.A.; Barman, S.R.; Chatterjee, S.; Khan, I.; Lin, Z.-H. Enhanced biosensing strategies using electrogenerated chemiluminescence: Recent progress and future prospects. *J. Mater. Chem. B* **2020**, *8*, 3192–3212. [CrossRef] [PubMed]
33. Qi, H.; Zhang, C. Electrogenerated Chemiluminescence Biosensing. *Anal. Chem.* **2020**, *92*, 524–534. [CrossRef] [PubMed]
34. Perera, G.S.; Ahmed, T.; Heiss, L.; Walia, S.; Bhaskaran, M.; Sriram, S. Rapid and Selective Biomarker Detection with Conductometric Sensors. *Small* **2021**, *17*, 2005582. [CrossRef]
35. Liu, R.; Ye, X.; Cui, T. Recent Progress of Biomarker Detection Sensors. *Research* **2020**, *2020*, 7949037. [CrossRef] [PubMed]
36. Shang, L.; Wang, X.; Zhang, W.; Jia, L.-P.; Ma, R.-N.; Jia, W.-L.; Wang, H.-S. A dual-potential electrochemiluminescence sensor for ratiometric detection of carcinoembryonic antigen based on single luminophor. *Sens. Actuators B Chem.* **2020**, *325*, 128776. [CrossRef]

37. Luo, W.; Ye, Z.; Ma, P.; Wu, Q.; Song, D. Preparation of a disposable electrochemiluminescence sensor chip based on an MXene-loaded ruthenium luminescent agent and its application in the detection of carcinoembryonic antigens. *Analyst* **2022**, *147*, 1986–1994. [CrossRef]
38. Shang, L.; Shi, B.-J.; Zhang, W.; Jia, L.-P.; Ma, R.-N.; Xue, Q.-W.; Wang, H.-S. Ratiometric Electrochemiluminescence Sensing of Carcinoembryonic Antigen Based on Luminol. *Anal. Chem.* **2022**, *94*, 12845–12851. [CrossRef]
39. Huang, B.; Liu, X.-P.; Chen, J.-S.; Mao, C.; Niu, H.-L.; Jin, B.-K. Electrochemiluminescence immunoassay for the prostate-specific antigen by using a CdS/chitosan/g-C_3N_4 nanocomposite. *Microchim. Acta* **2020**, *187*, 155. [CrossRef]
40. Wang, Y.; Feng, D.; Kan, X. The combination of highly efficient resonance energy transfer in one nanocomposite and ferrocene-quenching for ultrasensitive electrochemiluminescence bioanalysis. *Biosens. Bioelectron.* **2022**, *210*, 114347. [CrossRef]
41. Zheng, L.; Guo, Q.; Yang, C.; Wang, J.; Xu, X.; Nie, G. Electrochemiluminescence and photoelectrochemistry dual-signal immunosensor based on $Ru(bpy)_3^{2+}$-functionalized MOF for prostate-specific antigen sensitive detection. *Sens. Actuators B Chem.* **2023**, *379*, 133269. [CrossRef]
42. Chen, H.; Huang, J.; Zhang, R.; Yan, F. Dual-mode electrochemiluminescence and electrochemical sensor for alpha-fetoprotein detection in human serum based on vertically ordered mesoporous silica films. *Front. Chem.* **2022**, *10*, 1023998. [CrossRef] [PubMed]
43. Qin, D.; Jiang, X.; Mo, G.; Feng, J.; Deng, B. Boron nitride quantum dots as electrochemiluminescence coreactants of rGO@Au@Ru–SiO_2 for label-free detection of AFP in human serum. *Electrochim. Acta* **2020**, *335*, 135621. [CrossRef]
44. Liang, Z.; Liu, Y.; Zhang, Q.; Guo, Y.; Ma, Q. The high luminescent polydopamine nanosphere-based ECL biosensor with steric effect for MUC1 detection. *Chem. Eng. J.* **2020**, *385*, 123825. [CrossRef]
45. Huang, W.; Hu, G.-B.; Yao, L.-Y.; Yang, Y.; Liang, W.-B.; Yuan, R.; Xiao, D.-R. Matrix Coordination-Induced Electrochemiluminescence Enhancement of Tetraphenylethylene-Based Hafnium Metal–Organic Framework: An Electrochemiluminescence Chromophore for Ultrasensitive Electrochemiluminescence Sensor Construction. *Anal. Chem.* **2020**, *92*, 3380–3387. [CrossRef]
46. Huang, W.; Wang, Y.; Liang, W.-B.; Hu, G.-B.; Yao, L.-Y.; Yang, Y.; Zhou, K.; Yuan, R.; Xiao, D.-R. Two Birds with One Stone: Surface Functionalization and Delamination of Multilayered $Ti_3C_2T_x$ MXene by Grafting a Ruthenium(II) Complex to Achieve Conductivity-Enhanced Electrochemiluminescence. *Anal. Chem.* **2021**, *93*, 1834–1841. [CrossRef]
47. Zhao, L.; Wang, B.; Wang, C.; Fan, D.; Liu, X.; Wei, Q.; Ju, H.; Wu, D. Dual-strategy ECL biosensor based on rare Eu(II,III)-MOF as probe with antenna effect and sensitization for CYFRA 21-1 trace analysis. *Sens. Actuators B Chem.* **2023**, *377*, 133101. [CrossRef]
48. Jian, L.; Wang, X.; Hao, L.; Liu, Y.; Yang, H.; Zheng, X.; Feng, W. Electrochemiluminescence immunosensor for cytokeratin fragment antigen 21-1 detection using electrochemically mediated atom transfer radical polymerization. *Microchim. Acta* **2021**, *188*, 115. [CrossRef]
49. Xue, J.; Yang, L.; Du, Y.; Ren, Y.; Ren, X.; Ma, H.; Wu, D.; Ju, H.; Li, Y.; Wei, Q. Electrochemiluminescence sensing platform based on functionalized poly-(styrene-co-maleicanhydride) nanocrystals and iron doped hydroxyapatite for CYFRA 21-1 immunoassay. *Sens. Actuators B Chem.* **2020**, *321*, 128454. [CrossRef]
50. Li, J.; Yang, H.; Cai, R.; Tan, W. Ultrahighly Sensitive Sandwich-Type Electrochemical Immunosensor for Selective Detection of Tumor Biomarkers. *ACS Appl. Mater. Interfaces* **2022**, *14*, 44222–44227. [CrossRef]
51. Li, C.; Yang, J.; Xu, R.; Wang, H.; Zhang, Y.; Wei, Q. Progress and Prospects of Electrochemiluminescence Biosensors Based on Porous Nanomaterials. *Biosensors* **2022**, *12*, 508. [CrossRef] [PubMed]
52. Chen, X.; Liu, Y.; Wang, B.; Liu, X.; Lu, C. Understanding role of microstructures of nanomaterials in electrochemiluminescence properties and their applications. *TrAC Trends Anal. Chem.* **2023**, *162*, 117030. [CrossRef]
53. Padmakumari Kurup, C.; Abdullah Lim, S.; Ahmed, M.U. Nanomaterials as signal amplification elements in aptamer-based electrochemiluminescent biosensors. *Bioelectrochemistry* **2022**, *147*, 108170. [CrossRef]
54. Zou, G.; Ju, H. Electrogenerated Chemiluminescence from a CdSe Nanocrystal Film and Its Sensing Application in Aqueous Solution. *Anal. Chem.* **2004**, *76*, 6871–6876. [CrossRef]
55. Zhou, J.; Yang, Y.; Zhang, C. Toward Biocompatible Semiconductor Quantum Dots: From Biosynthesis and Bioconjugation to Biomedical Application. *Chem. Rev.* **2015**, *115*, 11669–11717. [CrossRef]
56. Zhang, X.; Zhang, B.; Miao, W.; Zou, G. Molecular-Counting-Free and Electrochemiluminescent Single-Molecule Immunoassay with Dual-Stabilizers-Capped CdSe Nanocrystals as Labels. *Anal. Chem.* **2016**, *88*, 5482–5488. [CrossRef]
57. Liu, S.; Zhang, X.; Yu, Y.; Zou, G. A Monochromatic Electrochemiluminescence Sensing Strategy for Dopamine with Dual-Stabilizers-Capped CdSe Quantum Dots as Emitters. *Anal. Chem.* **2014**, *86*, 2784–2788. [CrossRef]
58. Lin, D.; Wu, J.; Yan, F.; Deng, S.; Ju, H. Ultrasensitive Immunoassay of Protein Biomarker Based on Electrochemiluminescent Quenching of Quantum Dots by Hemin Bio-Bar-Coded Nanoparticle Tags. *Anal. Chem.* **2011**, *83*, 5214–5221. [CrossRef]
59. Fan, Y.; Liu, Z.; Wang, J.; Cui, C.; Hu, L. An "off–on" electrochemiluminescence aptasensor for determination of lincomycin based on CdS QDs/carboxylated g-C3N4. *Microchim. Acta* **2023**, *190*, 11. [CrossRef]
60. Chen, P.; Liu, Z.; Liu, J.; Liu, H.; Bian, W.; Tian, D.; Xia, F.; Zhou, C. A novel electrochemiluminescence aptasensor based CdTe QDs@NH_2-MIL-88(Fe) for signal amplification. *Electrochimica Acta* **2020**, *354*, 136644. [CrossRef]
61. Zhu, H.-Y.; Ding, S.-N. Dual-signal-amplified electrochemiluminescence biosensor for microRNA detection by coupling cyclic enzyme with CdTe QDs aggregate as luminophor. *Biosens. Bioelectron.* **2019**, *134*, 109–116. [CrossRef] [PubMed]
62. Zhao, J.; He, Y.; Tan, K.; Yang, J.; Chen, S.; Yuan, R. Novel Ratiometric Electrochemiluminescence Biosensor Based on BP-CdTe QDs with Dual Emission for Detecting MicroRNA-126. *Anal. Chem.* **2021**, *93*, 12400–12408. [CrossRef] [PubMed]

63. Wang, J.; Han, H.; Jiang, X.; Huang, L.; Chen, L.; Li, N. Quantum Dot-Based Near-Infrared Electrochemiluminescent Immunosensor with Gold Nanoparticle-Graphene Nanosheet Hybrids and Silica Nanospheres Double-Assisted Signal Amplification. *Anal. Chem.* **2012**, *84*, 4893–4899. [CrossRef] [PubMed]
64. Li, Z.; Lin, Z.; Wu, X.; Chen, H.; Chai, Y.; Yuan, R. Highly Efficient Electrochemiluminescence Resonance Energy Transfer System in One Nanostructure: Its Application for Ultrasensitive Detection of MicroRNA in Cancer Cells. *Anal. Chem.* **2017**, *89*, 6029–6035. [CrossRef] [PubMed]
65. Liu, Y.; Wang, F.; Ge, S.; Zhang, L.; Zhang, Z.; Liu, Y.; Zhang, Y.; Ge, S.; Yu, J. Programmable T-Junction Structure-Assisted CRISPR/Cas12a Electrochemiluminescence Biosensor for Detection of Sa-16S rDNA. *ACS Appl. Mater. Interfaces* **2023**, *15*, 617–625. [CrossRef]
66. Yang, E.; Zhang, Y.; Shen, Y. Quantum dots for electrochemiluminescence bioanalysis—A review. *Anal. Chim. Acta* **2022**, *1209*, 339140. [CrossRef]
67. Pan, D.; Chen, K.; Zhou, Q.; Zhao, J.; Xue, H.; Zhang, Y.; Shen, Y. Engineering of CdTe/SiO_2 nanocomposites: Enhanced signal amplification and biocompatibility for electrochemiluminescent immunoassay of alpha-fetoprotein. *Biosens. Bioelectron.* **2019**, *131*, 178–184. [CrossRef]
68. Shen, C.; Li, Y.; Li, Y.; Wang, S.; Li, Y.; Tang, F.; Wang, P.; Liu, H.; Li, Y.; Liu, Q. A double reaction system induced electrochemiluminescence enhancement based on SnS_2 QDs@MIL-101 for ultrasensitive detection of CA242. *Talanta* **2022**, *247*, 123575. [CrossRef]
69. Lei, Y.-M.; Zhou, J.; Chai, Y.-Q.; Zhuo, Y.; Yuan, R. SnS_2 Quantum Dots as New Emitters with Strong Electrochemiluminescence for Ultrasensitive Antibody Detection. *Anal. Chem.* **2018**, *90*, 12270–12277. [CrossRef]
70. Zhao, M.; Chen, A.-Y.; Huang, D.; Chai, Y.-Q.; Zhuo, Y.; Yuan, R. MoS_2 Quantum Dots as New Electrochemiluminescence Emitters for Ultrasensitive Bioanalysis of Lipopolysaccharide. *Anal. Chem.* **2017**, *89*, 8335–8342. [CrossRef]
71. Hua, Q.; Tang, F.; Wang, X.; Li, M.; Gu, X.; Sun, W.; Luan, F.; Tian, C.; Zhuang, X. Electrochemiluminescence sensor based on EuS nanocrystals for ultrasensitive detection of mercury ions in seafood. *Sens. Actuators B Chem.* **2022**, *352*, 131075. [CrossRef]
72. Jiang, D.; Wei, M.; Du, X.; Qin, M.; Shan, X.; Wang, W.; Chen, Z. Ultrasensitive near-infrared aptasensor for enrofloxacin detection based on wavelength tunable AgBr nanocrystals electrochemiluminescence emission triggered by O-terminated Ti_3C_2 MXene. *Biosens. Bioelectron.* **2022**, *200*, 113917. [CrossRef] [PubMed]
73. Lei, Y.-M.; Zhuo, Y.; Guo, M.-L.; Chai, Y.-Q.; Yuan, R. Pore Confinement-Enhanced Electrochemiluminescence on SnO_2 Nanocrystal Xerogel with NO_3^- As Co-Reactant and Its Application in Facile and Sensitive Bioanalysis. *Anal. Chem.* **2020**, *92*, 2839–2846. [CrossRef] [PubMed]
74. Yu, S.; Du, Y.; Niu, X.; Li, G.; Zhu, D.; Yu, Q.; Zou, G.; Ju, H. Arginine-modified black phosphorus quantum dots with dual excited states for enhanced electrochemiluminescence in bioanalysis. *Nat. Commun.* **2022**, *13*, 7302. [CrossRef]
75. Chen, J.; Wang, Q.; Liu, X.; Chen, X.; Wang, L.; Yang, W. Black phosphorus quantum dots as novel electrogenerated chemiluminescence emitters for the detection of Cu^{2+}. *Chem. Commun.* **2020**, *56*, 4680–4683. [CrossRef]
76. Li, P.; Yu, J.; Zhao, K.; Deng, A.; Li, J. Efficient enhancement of electrochemiluminescence from tin disulfide quantum dots by hollow titanium dioxide spherical shell for highly sensitive detection of chloramphenicol. *Biosens. Bioelectron.* **2020**, *147*, 111790. [CrossRef]
77. Fu, L.; Fu, K.; Gao, X.; Dong, S.; Zhang, B.; Fu, S.; Hsu, H.-Y.; Zou, G. Enhanced Near-Infrared Electrochemiluminescence from Trinary Ag–In–S to Multinary Ag–Ga–In–S Nanocrystals via Doping-in-Growth and Its Immunosensing Applications. *Anal. Chem.* **2021**, *93*, 2160–2165. [CrossRef]
78. Long, X.; Zhang, F.; He, Y.; Hou, S.; Zhang, B.; Zou, G. Promising Anodic Electrochemiluminescence of Nontoxic Core/Shell $CuInS_2$/ZnS Nanocrystals in Aqueous Medium and Its Biosensing Potential. *Anal. Chem.* **2018**, *90*, 3563–3569. [CrossRef]
79. Wang, C.; Liu, L.; Liu, X.; Chen, Y.; Wang, X.; Fan, D.; Kuang, X.; Sun, X.; Wei, Q.; Ju, H. Highly-sensitive electrochemiluminescence biosensor for NT-proBNP using MoS_2@Cu_2S as signal-enhancer and multinary nanocrystals loaded in mesoporous UiO-66-NH_2 as novel luminophore. *Sens. Actuators B Chem.* **2020**, *307*, 127619. [CrossRef]
80. Jiang, X.; Wang, H.; Shen, Y.; Hu, N.; Shi, W. Nitrogen-doped Ti_3C_2 MXene quantum dots as novel high-efficiency electrochemiluminescent emitters for sensitive mucin 1 detection. *Sens. Actuators B Chem.* **2022**, *350*, 130891. [CrossRef]
81. Chen, A.; Liang, W.; Wang, H.; Zhuo, Y.; Chai, Y.; Yuan, R. Anodic Electrochemiluminescence of Carbon Dots Promoted by Nitrogen Doping and Application to Rapid Cancer Cell Detection. *Anal. Chem.* **2020**, *92*, 1379–1385. [CrossRef]
82. Chen, Y.; Lin, J.; Zhang, R.; He, S.; Ding, Z.; Ding, L. Electrochemiluminescence of water-dispersed nitrogen and sulfur doped carbon dots synthesized from amino acids. *Analyst* **2021**, *146*, 5287–5293. [CrossRef]
83. Liu, J.; Zhang, Y.; Yuan, R.; Chai, Y. Fluorine-nitrogen co-doped carbon dots with stable and strong electrochemiluminescence as an emitter for ultrasensitive detection of HIV-DNA fragment. *Sens. Actuators B Chem.* **2023**, *379*, 133260. [CrossRef]
84. Yang, E.; Ning, Z.; Yin, F.; Fang, Z.; Chen, M.; Zhang, M.; Xu, W.; Zhang, Y.; Shen, Y. Surface plasmon-enhanced electrochemiluminescence of P, N-doped carbon dots for ultrasensitive detection of BRAF gene. *Sens. Actuators B Chem.* **2022**, *369*, 132288. [CrossRef]
85. Chen, S.; Jiang, L.; Yin, B.; Du, W.; Wang, X.; Liu, Y.; Chen, S.; Zhu, M. Bright Near-Infrared Circularly Polarized Electrochemiluminescence from Au_9Ag_4 Nanoclusters. *Chem. Sci.* **2023**, *14*, 7304–7309. [CrossRef]
86. Cao, Y.; Zhou, J.-L.; Ma, Y.; Zhou, Y.; Zhu, J.-J. Recent progress of metal nanoclusters in electrochemiluminescence. *Dalton Trans.* **2022**, *51*, 8927–8937. [CrossRef] [PubMed]

87. Han, S.; Zhao, Y.; Zhang, Z.; Xu, G. Recent Advances in Electrochemiluminescence and Chemiluminescence of Metal Nanoclusters. *Molecules* **2020**, *25*, 5208. [CrossRef] [PubMed]
88. Díez, I.; Pusa, M.; Kulmala, S.; Jiang, H.; Walther, A.; Goldmann, A.S.; Müller, A.H.E.; Ikkala, O.; Ras, R.H.A. Color Tunability and Electrochemiluminescence of Silver Nanoclusters. *Angew. Chem. Int. Ed.* **2009**, *48*, 2122–2125. [CrossRef]
89. Wang, T.; Wang, D.; Padelford, J.W.; Jiang, J.; Wang, G. Near-Infrared Electrogenerated Chemiluminescence from Aqueous Soluble Lipoic Acid Au Nanoclusters. *J. Am. Chem. Soc.* **2016**, *138*, 6380–6383. [CrossRef]
90. Li, L.; Liu, H.; Shen, Y.; Zhang, J.; Zhu, J.-J. Electrogenerated Chemiluminescence of Au Nanoclusters for the Detection of Dopamine. *Anal. Chem.* **2011**, *83*, 661–665. [CrossRef]
91. Fang, Y.-M.; Song, J.; Li, J.; Wang, Y.-W.; Yang, H.-H.; Sun, J.-J.; Chen, G.-N. Electrogenerated chemiluminescence from Au nanoclusters. *Chem. Commun.* **2011**, *47*, 2369–2371. [CrossRef] [PubMed]
92. Hesari, M.; Ding, Z. Efficient Near-Infrared Electrochemiluminescence from Au_{18} Nanoclusters. *Chem. Eur. J.* **2021**, *27*, 14821–14825. [CrossRef] [PubMed]
93. Hesari, M.; Ding, Z. Identifying Highly Photoelectrochemical Active Sites of Two Au_{21} Nanocluster Isomers toward Bright Near-Infrared Electrochemiluminescence. *J. Am. Chem. Soc.* **2021**, *143*, 19474–19485. [CrossRef] [PubMed]
94. Hesari, M.; Ma, H.; Ding, Z. Monitoring single Au_{38} nanocluster reactions via electrochemiluminescence. *Chem. Sci.* **2021**, *12*, 14540–14545. [CrossRef] [PubMed]
95. Li, D.; Sun, X.; Shao, N.; Zhang, G.; Li, S.; Zhou, H.; Wu, J.; Tian, Y. Crystal structure, optical properties and electrochemiluminescence of Cu(I), Ag(I) and Au(I) complexes that contain the cyanoacetic acid triphenylamine ligand. *Polyhedron* **2015**, *93*, 17–22. [CrossRef]
96. Zhu, M.-J.; Pan, J.-B.; Wu, Z.-Q.; Gao, X.-Y.; Zhao, W.; Xia, X.-H.; Xu, J.-J.; Chen, H.-Y. Electrogenerated Chemiluminescence Imaging of Electrocatalysis at a Single Au-Pt Janus Nanoparticle. *Angew. Chem. Int. Ed.* **2018**, *57*, 4010–4014. [CrossRef]
97. Qian, H.; Jiang, D.; Li, G.; Gayathri, C.; Das, A.; Gil, R.R.; Jin, R. Monoplatinum Doping of Gold Nanoclusters and Catalytic Application. *J. Am. Chem. Soc.* **2012**, *134*, 16159–16162. [CrossRef]
98. Chen, S.; Ma, H.; Padelford, J.W.; Qinchen, W.; Yu, W.; Wang, S.; Zhu, M.; Wang, G. Near Infrared Electrochemiluminescence of Rod-Shape 25-Atom AuAg Nanoclusters That Is Hundreds-Fold Stronger Than That of $Ru(bpy)_3$ Standard. *J. Am. Chem. Soc.* **2019**, *141*, 9603–9609. [CrossRef]
99. Tang, Y.; Xu, J.; Xiong, C.; Xiao, Y.; Zhang, X.; Wang, S. Enhanced electrochemiluminescence of gold nanoclusters via silver doping and their application for ultrasensitive detection of dopamine. *Analyst* **2019**, *144*, 2643–2648. [CrossRef]
100. Guo, Y.; Tian, L.; Wu, J.; Wu, Y.; Liu, Y.; Du, J.; Lu, X. A Highly Sensitive Electrochemiluminescence Spermine Biosensor Based on Au−Ag Bimetallic Nanoclusters. *Electroanalysis* **2021**, *33*, 2016–2024. [CrossRef]
101. Nie, Y.; Tao, X.; Zhang, H.; Chai, Y.; Yuan, R. Self-Assembly of Gold Nanoclusters into a Metal–Organic Framework with Efficient Electrochemiluminescence and Their Application for Sensitive Detection of Rutin. *Anal. Chem.* **2021**, *93*, 3445–3451. [CrossRef] [PubMed]
102. Luo, S.; Xiao, H.; Yang, S.; Liu, C.; Liang, J.; Tang, Y. Ultrasensitive detection of pentachlorophenol based on enhanced electrochemiluminescence of Au nanoclusters/graphene hybrids. *Sens. Actuators B Chem.* **2014**, *194*, 325–331. [CrossRef]
103. Yang, Y.; Wu, W.; Wang, Q.; Xiao, H.; Kuang, Y.; Liu, C. Novel anodic electrochemiluminescence system of Pt nanocluster/graphene hybrids for ultrasensitive detection of Cu^{2+}. *J. Electroanal. Chem.* **2016**, *772*, 73–79. [CrossRef]
104. Guo, C.; Duan, F.; Zhang, S.; He, L.; Wang, M.; Chen, J.; Zhang, J.; Jia, Q.; Zhang, Z.; Du, M. Heterostructured hybrids of metal–organic frameworks (MOFs) and covalent–organic frameworks (COFs). *J. Mater. Chem. A* **2022**, *10*, 475–507. [CrossRef]
105. Wang, Z.; Liu, L.; Li, Z.; Goyal, N.; Du, T.; He, J.; Li, G.K. Shaping of Metal–Organic Frameworks: A Review. *Energy Fuels* **2022**, *36*, 2927–2944. [CrossRef]
106. Hwang, J.; Ejsmont, A.; Freund, R.; Goscianska, J.; Schmidt, B.V.K.J.; Wuttke, S. Controlling the morphology of metal–organic frameworks and porous carbon materials: Metal oxides as primary architecture-directing agents. *Chem. Soc. Rev.* **2020**, *49*, 3348–3422. [CrossRef]
107. Wang, Y.; Zhao, G.; Chi, H.; Yang, S.; Niu, Q.; Wu, D.; Cao, W.; Li, T.; Ma, H.; Wei, Q. Self-Luminescent Lanthanide Metal–Organic Frameworks as Signal Probes in Electrochemiluminescence Immunoassay. *J. Am. Chem. Soc.* **2021**, *143*, 504–512. [CrossRef]
108. Dong, X.; Zhao, G.; Li, X.; Fang, J.; Miao, J.; Wei, Q.; Cao, W. Electrochemiluminescence immunosensor of "signal-off" for β-amyloid detection based on dual metal-organic frameworks. *Talanta* **2020**, *208*, 120376. [CrossRef]
109. Huang, W.; Hu, G.-B.; Liang, W.-B.; Wang, J.-M.; Lu, M.-L.; Yuan, R.; Xiao, D.-R. Ruthenium(II) Complex-Grafted Hollow Hierarchical Metal–Organic Frameworks with Superior Electrochemiluminescence Performance for Sensitive Assay of Thrombin. *Anal. Chem.* **2021**, *93*, 6239–6245. [CrossRef]
110. Zhu, X.; Xing, H.; Xue, Y.; Li, J.; Wang, E.; Dong, S. Atom-Anchoring Strategy with Metal–Organic Frameworks for Highly Efficient Solid-State Electrochemiluminescence. *Anal. Chem.* **2021**, *93*, 9628–9633. [CrossRef]
111. Zhao, G.; Wang, Y.; Li, X.; Dong, X.; Wang, H.; Du, B.; Cao, W.; Wei, Q. Quenching Electrochemiluminescence Immunosensor Based on Resonance Energy Transfer between Ruthenium (II) Complex Incorporated in the UiO-67 Metal–Organic Framework and Gold Nanoparticles for Insulin Detection. *ACS Appl. Mater. Interfaces* **2018**, *10*, 22932–22938. [CrossRef] [PubMed]
112. Dong, X.; Zhao, G.; Liu, L.; Li, X.; Wei, Q.; Cao, W. Ultrasensitive competitive method-based electrochemiluminescence immunosensor for diethylstilbestrol detection based on $Ru(bpy)_3^{2+}$ as luminophor encapsulated in metal–organic frameworks UiO-67. *Biosens. Bioelectron.* **2018**, *110*, 201–206. [CrossRef] [PubMed]

113. Wang, C.; Zhang, N.; Wei, D.; Feng, R.; Fan, D.; Hu, L.; Wei, Q.; Ju, H. Double electrochemiluminescence quenching effects of Fe_3O_4@PDA-Cu_XO towards self-enhanced $Ru(bpy)_3^{2+}$ functionalized MOFs with hollow structure and its application to procalcitonin immunosensing. *Biosens. Bioelectron.* **2019**, *142*, 111521. [CrossRef]
114. Dong, X.; Du, Y.; Zhao, G.; Cao, W.; Fan, D.; Kuang, X.; Wei, Q.; Ju, H. Dual-signal electrochemiluminescence immunosensor for Neuron-specific enolase detection based on "dual-potential" emitter $Ru(bpy)_3^{2+}$ functionalized zinc-based metal-organic frameworks. *Biosens. Bioelectron.* **2021**, *192*, 113505. [CrossRef] [PubMed]
115. Li, P.; Luo, L.; Cheng, D.; Sun, Y.; Zhang, Y.; Liu, M.; Yao, S. Regulation of the Structure of Zirconium-Based Porphyrinic Metal–Organic Framework as Highly Electrochemiluminescence Sensing Platform for Thrombin. *Anal. Chem.* **2022**, *94*, 5707–5714. [CrossRef] [PubMed]
116. Hu, G.-B.; Xiong, C.-Y.; Liang, W.-B.; Zeng, X.-S.; Xu, H.-L.; Yang, Y.; Yao, L.-Y.; Yuan, R.; Xiao, D.-R. Highly Stable Mesoporous Luminescence-Functionalized MOF with Excellent Electrochemiluminescence Property for Ultrasensitive Immunosensor Construction. *ACS Appl. Mater. Interfaces* **2018**, *10*, 15913–15919. [CrossRef]
117. Wang, Z.; Jiang, X.; Yuan, R.; Chai, Y. *N*-(aminobutyl)-*N*-(ethylisoluminol) functionalized Fe-based metal-organic frameworks with intrinsic mimic peroxidase activity for sensitive electrochemiluminescence mucin1 determination. *Biosens. Bioelectron.* **2018**, *121*, 250–256. [CrossRef]
118. Wang, C.; Zhang, N.; Li, Y.; Yang, L.; Wei, D.; Yan, T.; Ju, H.; Du, B.; Wei, Q. Cobalt-based metal-organic frameworks as co-reaction accelerator for enhancing electrochemiluminescence behavior of *N*-(aminobutyl)-*N*-(ethylisoluminol) and ultrasensitive immunosensing of amyloid-β protein. *Sens. Actuators B Chem.* **2019**, *291*, 319–328. [CrossRef]
119. Wang, S.; Zhao, Y.; Wang, M.; Li, H.; Saqib, M.; Ge, C.; Zhang, X.; Jin, Y. Enhancing Luminol Electrochemiluminescence by Combined Use of Cobalt-Based Metal Organic Frameworks and Silver Nanoparticles and Its Application in Ultrasensitive Detection of Cardiac Troponin I. *Anal. Chem.* **2019**, *91*, 3048–3054. [CrossRef]
120. Zhu, D.; Zhang, Y.; Bao, S.; Wang, N.; Yu, S.; Luo, R.; Ma, J.; Ju, H.; Lei, J. Dual Intrareticular Oxidation of Mixed-Ligand Metal–Organic Frameworks for Stepwise Electrochemiluminescence. *J. Am. Chem. Soc.* **2021**, *143*, 3049–3053. [CrossRef]
121. Wang, J.-M.; Yao, L.-Y.; Huang, W.; Yang, Y.; Liang, W.-B.; Yuan, R.; Xiao, D.-R. Overcoming Aggregation-Induced Quenching by Metal−Organic Framework for Electrochemiluminescence (ECL) Enhancement: Zn-PTC as a New ECL Emitter for Ultrasensitive MicroRNAs Detection. *ACS Appl. Mater. Interfaces* **2021**, *13*, 44079–44085. [CrossRef] [PubMed]
122. Wu, J.; Wang, A.; Liu, P.; Hou, Y.; Song, L.; Yuan, R.; Fu, Y. Sulfur-functionalized zirconium(IV)-based metal-organic frameworks relieves aggregation-caused quenching effect in efficient electrochemiluminescence sensor. *Sens. Actuators B Chem.* **2020**, *321*, 128531. [CrossRef]
123. Wang, Y.; Shu, J.; Lyu, A.; Wang, M.; Hu, C.; Cui, H. Zn^{2+}-Modified Nonmetal Porphyrin-Based Metal–Organic Frameworks with Improved Electrochemiluminescence for Nanoscale Exosome Detection. *ACS Appl. Nano Mater.* **2023**, *6*, 4214–4223. [CrossRef]
124. Han, Q.; Wang, C.; Liu, P.; Zhang, G.; Song, L.; Fu, Y. Achieving synergistically enhanced dual-mode electrochemiluminescent and electrochemical drug sensors via a multi-effect porphyrin-based metal-organic framework. *Sens. Actuators B Chem.* **2021**, *330*, 129388. [CrossRef]
125. Li, J.; Jia, H.; Ren, X.; Li, Y.; Liu, L.; Feng, R.; Ma, H.; Wei, Q. Dumbbell Plate-Shaped AIEgen-Based Luminescent MOF with High Quantum Yield as Self-Enhanced ECL Tags: Mechanism Insights and Biosensing Application. *Small* **2022**, *18*, 2106567. [CrossRef]
126. Xiong, X.; Xiong, C.; Gao, Y.; Xiao, Y.; Chen, M.-M.; Wen, W.; Zhang, X.; Wang, S. Tetraphenylethylene-Functionalized Metal–Organic Frameworks with Strong Aggregation-Induced Electrochemiluminescence for Ultrasensitive Analysis through a Multiple Convertible Resonance Energy Transfer System. *Anal. Chem.* **2022**, *94*, 7861–7867. [CrossRef]
127. Xiao, S.; Wang, X.; Yang, C.; Jiang, Y.; Zhen, S.; Huang, C.; Li, Y. Electrochemiluminescence Resonance Energy Transfer System Based on Silver Metal–Organic Frameworks as a Double-Amplified Emitter for Sensitive Detection of miRNA-107. *Anal. Chem.* **2022**, *94*, 1178–1186. [CrossRef]
128. Richter, M.M.; Bard, A.J. Electrogenerated Chemiluminescence. 58. Ligand-Sensitized Electrogenerated Chemiluminescence in Europium Labels. *Anal. Chem.* **1996**, *68*, 2641–2650. [CrossRef]
129. Dong, H.; Liu, S.; Liu, Q.; Li, Y.; Xu, Z.; Li, Y.; Wei, Q. Mixed-Ligand-Regulated Self-Enhanced Luminous Eu-MOF as an ECL Signal Probe for an Oriented Antibody-Decorated Biosensing Platform. *Anal. Chem.* **2022**, *94*, 12852–12859. [CrossRef]
130. Dai, W.; Wang, X.; Chen, G.; Wang, X.; Hu, C.; Zhen, S.; Huang, C.; Li, Y. Facile synthesis of 2D Europium-metal organic frameworks nanosheets for highly efficient electrochemiluminescence in DNA detection. *Chem. Eng. J.* **2023**, *465*, 143037. [CrossRef]
131. Zhao, L.; Song, X.; Ren, X.; Fan, D.; Wei, Q.; Wu, D. Rare Self-Luminous Mixed-Valence Eu-MOF with a Self-Enhanced Characteristic as a Near-Infrared Fluorescent ECL Probe for Nondestructive Immunodetection. *Anal. Chem.* **2021**, *93*, 8613–8621. [CrossRef]
132. Zhao, L.; Song, X.; Ren, X.; Wang, H.; Fan, D.; Wu, D.; Wei, Q. Ultrasensitive near-infrared electrochemiluminescence biosensor derived from Eu-MOF with antenna effect and high efficiency catalysis of specific CoS2 hollow triple shelled nanoboxes for procalcitonin. *Biosens. Bioelectron.* **2021**, *191*, 113409. [CrossRef] [PubMed]
133. Zhao, L.; Wang, M.; Song, X.; Liu, X.; Ju, H.; Ai, H.; Wei, Q.; Wu, D. Annihilation luminescent Eu-MOF as a near-infrared electrochemiluminescence probe for trace detection of trenbolone. *Chem. Eng. J.* **2022**, *434*, 134691. [CrossRef]

134. Wang, C.; Han, Q.; Liu, P.; Zhang, G.; Song, L.; Zou, X.; Fu, Y. A Superstable Luminescent Lanthanide Metal Organic Gel Utilized in an Electrochemiluminescence Sensor for Epinephrine Detection with a Narrow Potential Sweep Range. *ACS Sens.* **2021**, *6*, 252–258. [CrossRef] [PubMed]
135. Zhou, L.; Yang, L.; Wang, C.; Jia, H.; Xue, J.; Wei, Q.; Ju, H. Copper doped terbium metal organic framework as emitter for sensitive electrochemiluminescence detection of CYFRA 21-1. *Talanta* **2022**, *238*, 123047. [CrossRef]
136. Wang, C.; Li, Z.; Ju, H. Copper-Doped Terbium Luminescent Metal Organic Framework as an Emitter and a Co-reaction Promoter for Amplified Electrochemiluminescence Immunoassay. *Anal. Chem.* **2021**, *93*, 14878–14884. [CrossRef]
137. Gao, H.; Wei, X.; Li, M.; Wang, L.; Wei, T.; Dai, Z. Co-Quenching Effect between Lanthanum Metal–Organic Frameworks Luminophore and Crystal Violet for Enhanced Electrochemiluminescence Gene Detection. *Small* **2021**, *17*, 2103424. [CrossRef]
138. Wang, X.Y.; Xiao, S.Y.; Jiang, Z.W.; Zhen, S.J.; Huang, C.Z.; Liu, Q.Q.; Li, Y.F. An ultrathin 2D Yb(III) metal-organic frameworks with strong electrochemiluminescence as a "on-off-on" platform for detection of picric acid and berberine chloride form. *Talanta* **2021**, *234*, 122625. [CrossRef]
139. Li, C.; Liu, L.; Kang, J.; Xiao, Y.; Feng, Y.; Cao, F.-F.; Zhang, H. Pristine MOF and COF materials for advanced batteries. *Energy Storage Mater.* **2020**, *31*, 115–134. [CrossRef]
140. Ren, X.; Liao, G.; Li, Z.; Qiao, H.; Zhang, Y.; Yu, X.; Wang, B.; Tan, H.; Shi, L.; Qi, X.; et al. Two-dimensional MOF and COF nanosheets for next-generation optoelectronic applications. *Coord. Chem. Rev.* **2021**, *435*, 213781. [CrossRef]
141. Freund, R.; Zaremba, O.; Arnauts, G.; Ameloot, R.; Skorupskii, G.; Dincă, M.; Bavykina, A.; Gascon, J.; Ejsmont, A.; Goscianska, J.; et al. The Current Status of MOF and COF Applications. *Angew. Chem. Int. Ed.* **2021**, *60*, 23975–24001. [CrossRef]
142. Lv, X.; Li, Y.; Cui, B.; Fang, Y.; Wang, L. Electrochemiluminescent sensor based on an aggregation-induced emission probe for bioanalytical detection. *Analyst* **2022**, *147*, 2338–2354. [CrossRef]
143. Zhang, J.-L.; Yang, Y.; Liang, W.-B.; Yao, L.-Y.; Yuan, R.; Xiao, D.-R. Highly Stable Covalent Organic Framework Nanosheets as a New Generation of Electrochemiluminescence Emitters for Ultrasensitive MicroRNA Detection. *Anal. Chem.* **2021**, *93*, 3258–3265. [CrossRef]
144. Luo, R.; Lv, H.; Liao, Q.; Wang, N.; Yang, J.; Li, Y.; Xi, K.; Wu, X.; Ju, H.; Lei, J. Intrareticular charge transfer regulated electrochemiluminescence of donor–acceptor covalent organic frameworks. *Nat. Commun.* **2021**, *12*, 6808. [CrossRef] [PubMed]
145. Li, Y.-J.; Cui, W.-R.; Jiang, Q.-Q.; Wu, Q.; Liang, R.-P.; Luo, Q.-X.; Qiu, J.-D. A general design approach toward covalent organic frameworks for highly efficient electrochemiluminescence. *Nat. Commun.* **2021**, *12*, 4735. [CrossRef] [PubMed]
146. Cui, W.-R.; Li, Y.-J.; Jiang, Q.-Q.; Wu, Q.; Luo, Q.-X.; Zhang, L.; Liang, R.-P.; Qiu, J.-D. Covalent Organic Frameworks as Advanced Uranyl Electrochemiluminescence Monitoring Platforms. *Anal. Chem.* **2021**, *93*, 16149–16157. [CrossRef]
147. Li, Y.-J.; Cui, W.-R.; Jiang, Q.-Q.; Liang, R.-P.; Li, X.-J.; Wu, Q.; Luo, Q.-X.; Liu, J.; Qiu, J.-D. Arousing Electrochemiluminescence Out of Non-Electroluminescent Monomers within Covalent Organic Frameworks. *ACS Appl. Mater. Interfaces* **2021**, *13*, 47921–47931. [CrossRef] [PubMed]
148. Zhang, J.-L.; Yao, L.-Y.; Yang, Y.; Liang, W.-B.; Yuan, R.; Xiao, D.-R. Conductive Covalent Organic Frameworks with Conductivity- and Pre-Reduction-Enhanced Electrochemiluminescence for Ultrasensitive Biosensor Construction. *Anal. Chem.* **2022**, *94*, 3685–3692. [CrossRef]
149. Qin, X.; Zhan, Z.; Ding, Z. Progress in electrochemiluminescence biosensors based on organic framework emitters. *Curr. Opin. Electrochem.* **2023**, *39*, 101283. [CrossRef]
150. Hisaki, I.; Xin, C.; Takahashi, K.; Nakamura, T. Designing Hydrogen-Bonded Organic Frameworks (HOFs) with Permanent Porosity. *Angew. Chem. Int. Ed.* **2019**, *58*, 11160–11170. [CrossRef] [PubMed]
151. Hou, H.; Wang, Y.; Wang, Y.; Luo, R.; Zhu, D.; Zhou, J.; Wu, X.; Ju, H.; Lei, J. Intrareticular electron coupling pathway driven electrochemiluminescence in hydrogen-bonded organic frameworks. *J. Mater. Chem. C* **2022**, *10*, 14488–14495. [CrossRef]
152. Shen, K.-Y.; Zhan, J.; Shen, L.; Xiong, Z.; Zhu, H.-T.; Wang, A.-J.; Yuan, P.-X.; Feng, J.-J. Hydrogen Bond Organic Frameworks as Radical Reactors for Enhancement in ECL Efficiency and Their Ultrasensitive Biosensing. *Anal. Chem.* **2023**, *95*, 4735–4743. [CrossRef] [PubMed]
153. Chang, Y.-L.; Palacios, R.E.; Fan, F.-R.F.; Bard, A.J.; Barbara, P.F. Electrogenerated Chemiluminescence of Single Conjugated Polymer Nanoparticles. *J. Am. Chem. Soc.* **2008**, *130*, 8906–8907. [CrossRef]
154. Bai, X.; Wang, K.; Chen, L.; Zhou, J.; Wang, J. Semiconducting polymer dots as fluorescent probes for in vitro biosensing. *J. Mater. Chem. B* **2022**, *10*, 6248–6262. [CrossRef] [PubMed]
155. Yuan, Y.; Hou, W.; Qin, W.; Wu, C. Recent advances in semiconducting polymer dots as optical probes for biosensing. *Biomater. Sci.* **2021**, *9*, 328–346. [CrossRef] [PubMed]
156. Feng, Y.; Wang, N.; Ju, H. Electrochemiluminescence biosensing and bioimaging with nanomaterials as emitters. *Sci. China Chem.* **2022**, *65*, 2417–2436. [CrossRef]
157. Wang, Z.; Guo, H.; Luo, Z.; Duan, Y.; Feng, Y. Low-Triggering-Potential Electrochemiluminescence from a Luminol Analogue Functionalized Semiconducting Polymer Dots for Imaging Detection of Blood Glucose. *Anal. Chem.* **2022**, *94*, 5615–5623. [CrossRef]
158. Dai, R.; Wu, F.; Xu, H.; Chi, Y. Anodic, Cathodic, and Annihilation Electrochemiluminescence Emissions from Hydrophilic Conjugated Polymer Dots in Aqueous Medium. *ACS Appl. Mater. Interfaces* **2015**, *7*, 15160–15167. [CrossRef]
159. Feng, Y.; Wang, N.; Ju, H. Highly Efficient Electrochemiluminescence of Cyanovinylene-Contained Polymer Dots in Aqueous Medium and Its Application in Imaging Analysis. *Anal. Chem.* **2018**, *90*, 1202–1208. [CrossRef]

160. Wang, N.; Feng, Y.; Wang, Y.; Ju, H.; Yan, F. Electrochemiluminescent Imaging for Multi-immunoassay Sensitized by Dual DNA Amplification of Polymer Dot Signal. *Anal. Chem.* **2018**, *90*, 7708–7714. [CrossRef]
161. Zhao, J.; Luo, J.; Liu, D.; He, Y.; Li, Q.; Chen, S.; Yuan, R. A coreactant-free electrochemiluminescence (ECL) biosensor based on in situ generating quencher for the ultrasensitive detection of microRNA. *Sens. Actuators B Chem.* **2020**, *316*, 128139. [CrossRef]
162. Luo, J.-H.; Li, Q.; Chen, S.-H.; Yuan, R. Coreactant-Free Dual Amplified Electrochemiluminescent Biosensor Based on Conjugated Polymer Dots for the Ultrasensitive Detection of MicroRNA. *ACS Appl. Mater. Interfaces* **2019**, *11*, 27363–27370. [CrossRef]
163. Liu, D.; Zhang, X.; Zhao, J.; Chen, S.; Yuan, R. An ultrasensitive sensing platform for microRNA-155 based on H_2O_2 quenched hydroxide-dependent ECL emission of PFO Pdots. *Biosens. Bioelectron.* **2020**, *150*, 111872. [CrossRef]
164. Yang, H.; Wang, H.; Xiong, C.; Chai, Y.; Yuan, R. Highly sensitive electrochemiluminescence immunosensor based on ABEI/H_2O_2 system with PFO dots as enhancer for detection of kidney injury molecule-1. *Biosens. Bioelectron.* **2018**, *116*, 16–22. [CrossRef]
165. Feng, Y.; Sun, F.; Wang, N.; Lei, J.; Ju, H. Ru(bpy)$_3^{2+}$ Incorporated Luminescent Polymer Dots: Double-Enhanced Electrochemiluminescence for Detection of Single-Nucleotide Polymorphism. *Anal. Chem.* **2017**, *89*, 7659–7666. [CrossRef] [PubMed]
166. Wang, N.; Chen, L.; Chen, W.; Ju, H. Potential- and Color-Resolved Electrochemiluminescence of Polymer Dots for Array Imaging of Multiplex MicroRNAs. *Anal. Chem.* **2021**, *93*, 5327–5333. [CrossRef] [PubMed]
167. Wang, N.; Gao, H.; Li, Y.; Li, G.; Chen, W.; Jin, Z.; Lei, J.; Wei, Q.; Ju, H. Dual Intramolecular Electron Transfer for In Situ Coreactant-Embedded Electrochemiluminescence Microimaging of Membrane Protein. *Angew. Chem. Int. Ed.* **2021**, *60*, 197–201. [CrossRef]
168. Wang, Z.; Pan, J.; Li, Q.; Zhou, Y.; Yang, S.; Xu, J.; Hua, D. Improved AIE-Active Probe with High Sensitivity for Accurate Uranyl Ion Monitoring in the Wild Using Portable Electrochemiluminescence System for Environmental Applications. *Adv. Funct. Mater.* **2020**, *30*, 2000220. [CrossRef]
169. Zhang, N.; Gao, H.; Jia, Y.-L.; Pan, J.-B.; Luo, X.-L.; Chen, H.-Y.; Xu, J.-J. Ultrasensitive Nucleic Acid Assay Based on AIE-Active Polymer Dots with Excellent Electrochemiluminescence Stability. *Anal. Chem.* **2021**, *93*, 6857–6864. [CrossRef]
170. Wang, C.; Liu, S.; Ju, H. Electrochemiluminescence nanoemitters for immunoassay of protein biomarkers. *Bioelectrochemistry* **2023**, *149*, 108281. [CrossRef] [PubMed]
171. Zhang, N.; Zhao, Z.-Y.; Gao, H.; Yu, Y.; Pan, J.-B.; Chen, H.-Y.; Xu, J.-J. An ultrasensitive electrochemiluminescence assay for nucleic acid detection based on carboxyl functionalized polymer dots. *J. Electroanal. Chem.* **2021**, *900*, 115743. [CrossRef]
172. Gao, H.; Zhang, N.; Hu, J.; Pan, J.-B.; Cheng, Y.-X.; Chen, H.-Y.; Xu, J.-J. Molecular Engineering of Polymer Dots for Electrochemiluminescence Emission. *ACS Appl. Nano Mater.* **2021**, *4*, 7244–7252. [CrossRef]
173. Khan, H.; Shah, M.R.; Barek, J.; Malik, M.I. Cancer biomarkers and their biosensors: A comprehensive review. *TrAC Trends Anal. Chem.* **2023**, *158*, 116813. [CrossRef]
174. Liu, X.; Zhao, S.; Tan, L.; Tan, Y.; Wang, Y.; Ye, Z.; Hou, C.; Xu, Y.; Liu, S.; Wang, G. Frontier and hot topics in electrochemiluminescence sensing technology based on CiteSpace bibliometric analysis. *Biosens. Bioelectron.* **2022**, *201*, 113932. [CrossRef]
175. Surinova, S.; Schiess, R.; Hüttenhain, R.; Cerciello, F.; Wollscheid, B.; Aebersold, R. On the Development of Plasma Protein Biomarkers. *J. Proteome Res.* **2011**, *10*, 5–16. [CrossRef]
176. Schwarzenbach, H.; Hoon, D.S.B.; Pantel, K. Cell-free nucleic acids as biomarkers in cancer patients. *Nat. Rev. Cancer* **2011**, *11*, 426–437. [CrossRef]
177. Binotti, W.W.; Bayraktutar, B.; Ozmen, M.C.; Cox, S.M.; Hamrah, P. A Review of Imaging Biomarkers of the Ocular Surface. *Eye Contact Lens Sci. Clin. Pract.* **2020**, *46*, S84–S105. [CrossRef]
178. Gao, X.; Liu, X.; Zeng, Y.; Zhang, Q.; Zhang, B.; Zou, G. Spectrum-Resolved Electrochemiluminescence to Multiplex the Immunoassay and DNA Probe Assay. *Anal. Chem.* **2022**, *94*, 15801–15808. [CrossRef] [PubMed]
179. Zhang, X.; Wang, Z.-J.; Wang, X.; Zhang, Y.-H.; Qu, J.; Ding, S.-N. Band-Edge Effect-Induced Electrochemiluminescence Signal Amplification Based on Inverse Opal Photonic Crystals for Ultrasensitive Detection of Carcinoembryonic Antigen. *Anal. Chem.* **2022**, *94*, 9919–9926. [CrossRef]
180. Huang, Y.; Lei, J.; Cheng, Y.; Ju, H. Ratiometric electrochemiluminescent strategy regulated by electrocatalysis of palladium nanocluster for immunosensing. *Biosens. Bioelectron.* **2016**, *77*, 733–739. [CrossRef] [PubMed]
181. Wu, M.-S.; Yuan, D.-J.; Xu, J.-J.; Chen, H.-Y. Electrochemiluminescence on bipolar electrodes for visual bioanalysis. *Chem. Sci.* **2013**, *4*, 1182–1188. [CrossRef]
182. Li, X.; Qin, X.; Tian, Z.; Wang, K.; Xia, X.; Wu, Y.; Liu, S. Gold Nanowires Array-Based Closed Bipolar Nanoelectrode System for Electrochemiluminescence Detection of α-Fetoprotein on Cell Surface. *Anal. Chem.* **2022**, *94*, 7350–7357. [CrossRef] [PubMed]
183. Yu, L.; Zhang, Q.; Kang, Q.; Zhang, B.; Shen, D.; Zou, G. Near-Infrared Electrochemiluminescence Immunoassay with Biocompatible Au Nanoclusters as Tags. *Anal. Chem.* **2020**, *92*, 7581–7587. [CrossRef]
184. Wang, Y.; Kan, X. Sensitive and selective "signal-off" electrochemiluminescence sensing of prostate-specific antigen based on an aptamer and molecularly imprinted polymer. *Analyst* **2021**, *146*, 7693–7701. [CrossRef]
185. Qin, D.; Meng, S.; Wu, Y.; Mo, G.; Deng, B. Aggregation-induced electrochemiluminescence resonance energy transfer with dual quenchers for the sensitive detection of prostate-specific antigen. *Sens. Actuators B Chem.* **2022**, *367*, 132176. [CrossRef]
186. Zhao, L.; Song, X.; Fan, D.; Liu, X.; Wang, H.; Wei, Q.; Wu, D. Highly Efficient Signal On/Off Electrochemiluminescence Gel Aptasensor Based on a Controlled Release Strategy for the Sensitive Detection of Prostate Specific Antigen. *Anal. Chem.* **2023**, *95*, 5695–5701. [CrossRef]

187. Fu, L.; Gao, X.; Dong, S.; Jia, J.; Xu, Y.; Wang, D.; Zou, G. Coreactant-Free and Direct Electrochemiluminescence from Dual-Stabilizer-Capped InP/ZnS Nanocrystals: A New Route Involving n-Type Luminophore. *Anal. Chem.* **2022**, *94*, 1350–1356. [CrossRef] [PubMed]
188. Yang, L.; Wu, T.; Du, Y.; Zhang, N.; Feng, R.; Ma, H.; Wei, Q. PEGylation Improved Electrochemiluminescence Supramolecular Assembly of Iridium(III) Complexes in Apoferritin for Immunoassays Using 2D/2D MXene/TiO_2 Hybrids as Signal Amplifiers. *Anal. Chem.* **2021**, *93*, 16906–16914. [CrossRef]
189. Yang, L.; Du, Y.; Fan, D.; Zhang, Y.; Kuang, X.; Sun, X.; Wei, Q. Facile Encapsulation of Iridium(III) Complexes in Apoferritin Nanocages as Promising Electrochemiluminescence Nanodots for Immunoassays. *Anal. Chem.* **2021**, *93*, 11329–11336. [CrossRef]
190. Han, Y.; Jia, Y.; Du, Y.; Li, Y.; Ren, X.; Ma, H.; Wu, D.; Kuang, X.; Fan, D.; Wei, Q. Controlled Growth of MoS_2 on Dendritic Ferric Oxide to Enhance Electrochemiluminescence of Nitrogen-Doped Carbon Quantum Dots for Sensitive Immunoassay. *Anal. Chem.* **2023**, *95*, 6655–6663. [CrossRef]
191. Du, Y.; Xue, J.; Sun, X.; Wu, D.; Liu, X.; Ju, H.; Yang, L.; Wei, Q. Oxygen Vacancy-Enhanced Electrochemiluminescence Sensing Strategy Using Luminol Thermally Encapsulated in Apoferritin as a Transducer for Biomarker Immunoassay. *Anal. Chem.* **2020**, *92*, 8472–8479. [CrossRef]
192. Xue, J.; Jia, Y.; Yang, L.; Feng, J.; Wu, D.; Ren, X.; Du, Y.; Ju, H.; Wei, Q. Etching Triangular Silver Nanoparticles by Self-generated Hydrogen Peroxide to Initiate the Response of an Electrochemiluminescence Sensing Platform. *Anal. Chem.* **2020**, *92*, 14203–14209. [CrossRef] [PubMed]
193. Yang, L.; Sun, X.; Wei, D.; Ju, H.; Du, Y.; Ma, H.; Wei, Q. Aggregation-Induced Electrochemiluminescence Bioconjugates of Apoferritin-Encapsulated Iridium(III) Complexes for Biosensing Application. *Anal. Chem.* **2021**, *93*, 1553–1560. [CrossRef] [PubMed]
194. Li, X.; Du, Y.; Wang, H.; Ma, H.; Wu, D.; Ren, X.; Wei, Q.; Xu, J.-J. Self-Supply of H_2O_2 and O_2 by Hydrolyzing CaO_2 to Enhance the Electrochemiluminescence of Luminol Based on a Closed Bipolar Electrode. *Anal. Chem.* **2020**, *92*, 12693–12699. [CrossRef] [PubMed]
195. Luo, Q.; Qian, X.; Mi, X.; Tu, Y. A novel electrochemiluminescent immunosensor for the detection of NT-proBNP based on a Au/ZIF-67 nanocomposite. *J. Electroanal. Chem.* **2022**, *912*, 116260. [CrossRef]
196. Yang, L.; Jia, Y.; Wu, D.; Zhang, Y.; Ju, H.; Du, Y.; Ma, H.; Wei, Q. Synthesis and Application of CeO_2/SnS_2 Heterostructures as a Highly Efficient Coreaction Accelerator in the Luminol–Dissolved O_2 System for Ultrasensitive Biomarkers Immunoassay. *Anal. Chem.* **2019**, *91*, 14066–14073. [CrossRef]
197. Jia, Y.; Yang, L.; Feng, R.; Ma, H.; Fan, D.; Yan, T.; Feng, R.; Du, B.; Wei, Q. $MnCO_3$ as a New Electrochemiluminescence Emitter for Ultrasensitive Bioanalysis of β-Amyloid$_{1–42}$ Oligomers Based on Site-Directed Immobilization of Antibody. *ACS Appl. Mater. Interfaces* **2019**, *11*, 7157–7163. [CrossRef]
198. Tan, R.; Wang, Y.; Mi, X.; Li, H.; Tu, Y. A dual-screening electrochemiluminescent aptasensor based on a mesoporous silica nano-sieve for specific detection of amyloid-β monomer. *Sens. Actuators B Chem.* **2022**, *352*, 131065. [CrossRef]
199. Ali, A.; Zhao, J.; Khan, M.S.; Wang, H.; Ren, X.; Hu, L.; Manzoor, R.; Wu, D.; Wei, Q. Electrochemiluminescence detection for β-amyloid$_{1\text{-}42}$ oligomers using silver nanoparticle decorated CuS@CoS_2 double shelled nanoboxes as dual-quencher. *Sens. Actuators B Chem.* **2021**, *329*, 129155. [CrossRef]
200. Qin, D.; Meng, S.; Wu, Y.; Mo, G.; Jiang, X.; Deng, B. Design of a Dual-Wavelength Ratiometric Electrochemiluminescence Immunosensor for Sensitive Detection of Amyloid-β Protein in Human Serum. *ACS Sustain. Chem. Eng.* **2021**, *9*, 7541–7549. [CrossRef]
201. Xu, M.-R.; Dai, R.-F.; Wei, Q.-Q.; Wang, J.; Feng, Y.-Y.; Hu, Y. Urinary AD7c-NTP Evaluates Cognition Impairment and Differentially Diagnoses AD and MCI. *Am. J. Alzheimers Dis. Dement.* **2022**, *37*, 153331752211152. [CrossRef]
202. Liang, Y.; Xue, K.; Shi, Y.; Zhan, T.; Lai, W.; Zhang, C. Dry Chemistry-Based Bipolar Electrochemiluminescence Immunoassay Device for Point-of-Care Testing of Alzheimer-Associated Neuronal Thread Protein. *Anal. Chem.* **2023**, *95*, 3434–3441. [CrossRef] [PubMed]
203. Domenico, T.; Rita, A.; Giacomo, S.; Diego, A.; Thelma, P.; Mariana, G.; Giampaolo, N.; Francesco, N.; Maria, G.; Francesco, F.; et al. Salivary biomarkers for diagnosis of acute myocardial infarction: A systematic review. *Int. J. Cardiol.* **2023**, *371*, 54–64. [CrossRef] [PubMed]
204. Gumanova, N.G.; Bogdanova, N.L.; Metelskaya, V.A.; Tarasov, V.I.; Kots, A.Y.; Kutsenko, V.A.; Kontsevaya, A.V.; Drapkina, O.M. Serum biomarkers, including nitric oxide metabolites (NOx), for prognosis of cardiovascular death and acute myocardial infarction in an ESSE-RF case–control cohort with 6.5-year follow up. *Sci. Rep.* **2022**, *12*, 18177. [CrossRef] [PubMed]
205. Yang, X.; Xu, Y.; Huang, X.; Hang, J.; Guo, W.; Dai, Z. Multicolor Iridium(III) Complexes with Host–Guest Recognition Motifs for Enhanced Electrochemiluminescence and Modular Labeling. *Anal. Chem.* **2023**, *95*, 4543–4549. [CrossRef]
206. Hong, D.; Kim, K.; Jo, E.-J.; Kim, M.-G. Electrochemiluminescence-Incorporated Lateral Flow Immunosensors Using $Ru(bpy)_3^{2+}$-Labeled Gold Nanoparticles for the Full-Range Detection of Physiological C-Reactive Protein Levels. *Anal. Chem.* **2021**, *93*, 7925–7932. [CrossRef]
207. Guo, X.-M.; Zhao, M.-L.; Liang, W.-B.; Yang, X.; Yuan, R.; Zhuo, Y. Programmable Y-Shaped Probes with Proximity Bivalent Recognition for Rapid Electrochemiluminescence Response of Acute Myocardial Infarction. *ACS Sens.* **2022**, *7*, 3208–3215. [CrossRef]

208. Ji, Y.; He, S.; Chen, Y.; Zhang, P.; Sun, J.; Li, Y.; Kuang, K.; Jia, N. A sensitive dual-signal electrochemiluminescence immunosensor based on $Ru(bpy)_3^{2+}$ @HKUST-1 and $Ce_2Sn_2O_7$ for detecting the heart failure biomarker NT-proBNP. *J. Mater. Chem. B* **2023**, *11*, 2754–2761. [CrossRef]
209. Xu, P.; Zhang, Y.; Li, X.; Ren, X.; Fan, D.; Wang, H.; Wei, Q.; Ju, H. Electrochemiluminescence immunosensor based on ferrocene functionalized ZIF-8 quenching the electrochemiluminescence of $Ru(bpy)_3^{2+}$-doped silica nanoparticles embodied *N*-butyldiethanolamine. *Sens. Actuators B Chem.* **2021**, *329*, 129101. [CrossRef]
210. Song, C.; Li, X.; Hu, L.; Shi, T.; Wu, D.; Ma, H.; Zhang, Y.; Fan, D.; Wei, Q.; Ju, H. Quench-Type Electrochemiluminescence Immunosensor Based on Resonance Energy Transfer from Carbon Nanotubes and Au-Nanoparticles-Enhanced g-C_3N_4 to CuO@Polydopamine for Procalcitonin Detection. *ACS Appl. Mater. Interfaces* **2020**, *12*, 8006–8015. [CrossRef]
211. Wang, N.; Yang, J.; Luo, Z.; Qin, D.; Wu, Y.; Deng, B. A dual-emitting immunosensor based on manganese dioxide nanoflowers and zinc sulfide quantum dots with enhanced electrochemiluminescence performance for the ultrasensitive detection of procalcitonin. *Analyst* **2023**, *148*, 2122–2132. [CrossRef] [PubMed]
212. Song, X.; Zhao, L.; Zhang, N.; Liu, L.; Ren, X.; Ma, H.; Kuang, X.; Li, Y.; Luo, C.; Wei, Q. Ultrasensitive Electrochemiluminescence Biosensor with Silver Nanoclusters as a Novel Signal Probe and α-Fe_2O_3–Pt as an Efficient Co-reaction Accelerator for Procalcitonin Immunoassay. *Anal. Chem.* **2023**, *95*, 1582–1588. [CrossRef] [PubMed]
213. Zhu, H.; Jiang, D.; Zhu, J.-J. High-resolution imaging of catalytic activity of a single graphene sheet using electrochemiluminescence microscopy. *Chem. Sci.* **2021**, *12*, 4794–4799. [CrossRef]
214. Knezevic, S.; Bouffier, L.; Liu, B.; Jiang, D.; Sojic, N. Electrochemiluminescence microscopy: From single objects to living cells. *Curr. Opin. Electrochem.* **2022**, *35*, 101096. [CrossRef]
215. Zhou, Y.; Dong, J.; Zhao, P.; Zhang, J.; Zheng, M.; Feng, J. Imaging of Single Bacteria with Electrochemiluminescence Microscopy. *J. Am. Chem. Soc.* **2023**, *145*, 8947–8953. [CrossRef]
216. Zhang, H.; Liu, Y.; Yao, M.; Han, W.; Zhang, S. Cathodic Electrochemiluminesence Microscopy for Imaging of Single Carbon Nanotube and Nucleolin at Single Tumor Cell. *Anal. Chem.* **2023**, *95*, 570–574. [CrossRef]
217. Lu, Y.; Huang, X.; Wang, S.; Li, B.; Liu, B. Nanoconfinement-Enhanced Electrochemiluminescence for in Situ Imaging of Single Biomolecules. *ACS Nano* **2023**, *17*, 3809–3817. [CrossRef]
218. Liu, G.; Jin, B.-K.; Ma, C.; Chen, Z.; Zhu, J.-J. Potential-Resolved Electrochemiluminescence Nanoprobes for Visual Apoptosis Evaluation at Single-Cell Level. *Anal. Chem.* **2019**, *91*, 6363–6370. [CrossRef]
219. Chen, Y.; Gou, X.; Ma, C.; Jiang, D.; Zhu, J.-J. A Synergistic Coreactant for Single-Cell Electrochemiluminescence Imaging: Guanine-Rich ssDNA-Loaded High-Index Faceted Gold Nanoflowers. *Anal. Chem.* **2021**, *93*, 7682–7689. [CrossRef] [PubMed]
220. Zhang, J.; Jin, R.; Jiang, D.; Chen, H.-Y. Electrochemiluminescence-Based Capacitance Microscopy for Label-Free Imaging of Antigens on the Cellular Plasma Membrane. *J. Am. Chem. Soc.* **2019**, *141*, 10294–10299. [CrossRef]
221. Chen, M.; Xu, C.; Zhao, W.; Chen, H.; Xu, J. Single Cell Imaging of Electrochemiluminescence-Driven Photodynamic Therapy. *Angew. Chem. Int. Ed.* **2022**, *61*, e2021174. [CrossRef]
222. Ding, H.; Guo, W.; Su, B. Imaging Cell-Matrix Adhesions and Collective Migration of Living Cells by Electrochemiluminescence Microscopy. *Angew. Chem. Int. Ed.* **2020**, *59*, 449–456. [CrossRef] [PubMed]
223. Ding, L.; Ding, H.; Zhou, P.; Xi, L.; Su, B. Surface-Sensitive Imaging Analysis of Cell–Microenvironment Interactions by Electrochemiluminescence Microscopy. *Anal. Chem.* **2022**, *94*, 10885–10892. [CrossRef] [PubMed]

Disclaimer/Publisher's Note: The statements, opinions and data contained in all publications are solely those of the individual author(s) and contributor(s) and not of MDPI and/or the editor(s). MDPI and/or the editor(s) disclaim responsibility for any injury to people or property resulting from any ideas, methods, instructions or products referred to in the content.